Quantitative Proteomics of a Chloroplast *SRP54* Sorting Mutant and Its Genetic Interactions with *CLPC1* in Arabidopsis[1][C][W][OA]

Heidi Rutschow[2], A. Jimmy Ytterberg[2,3], Giulia Friso, Robert Nilsson[4], and Klaas J. van Wijk*

Department of Plant Biology, Cornell University, Ithaca, New York 14853

cpSRP54 (for chloroplast SIGNAL RECOGNITION PARTICLE54) is involved in cotranslational and posttranslational sorting of thylakoid proteins. The Arabidopsis (*Arabidopsis thaliana*) cpSRP54 null mutant, *ffc1-2*, is pale green with delayed development. Western-blot analysis of individual leaves showed that the SRP sorting pathway, but not the SecY/E translocon, was strongly down-regulated with progressive leaf development in both wild-type and *ffc1-2* plants. To further understand the impact of cpSRP54 deletion, a quantitative comparison of *ffc2-1* was carried out for total leaf proteomes of young seedlings and for chloroplast proteomes of fully developed leaves using stable isotope labeling (isobaric stable isotope labeling and isotope-coded affinity tags) and two-dimensional gels. This showed that cpSRP54 deletion led to a change in light-harvesting complex composition, an increase of PsbS, and a decreased photosystem I/II ratio. Moreover, the cpSRP54 deletion led in young leaves to up-regulation of thylakoid proteases and stromal chaperones, including ClpC. In contrast, the stromal protein homeostasis machinery returned to wild-type levels in mature leaves, consistent with the developmental down-regulation of the SRP pathway. A differential response between young and mature leaves was also found in carbon metabolism, with an up-regulation of the Calvin cycle and the photorespiratory pathway in peroxisomes and mitochondria in young leaves but not in old leaves. The Calvin cycle was down-regulated in mature leaves to adjust to the reduced capacity of the light reaction, while reactive oxygen species defense proteins were up-regulated. The significance of ClpC up-regulation was confirmed through the generation of an *ffc2-1 clpc1* double mutant. This mutant was seedling lethal under autotrophic conditions but could be partially rescued under heterotrophic conditions.

Chloroplasts are essential for plant growth and development. Nucleus-encoded chloroplast proteins are imported into the chloroplast via the Tic/Toc complexes (Jarvis and Robinson, 2004; Soll and Schleiff, 2004; Kessler and Schnell, 2006), followed by processing, folding, and assembly by various chaperone systems. Proteins destined for the thylakoid membrane or the thylakoid lumen are targeted by four different sorting pathways that can be distinguished based on their energy requirements and protein components (Mori and Cline, 2001; Schunemann, 2007; Jarvis, 2008).

One of these posttranslational pathways is the signal recognition particle (SRP) pathway, which targets specific members of the LIGHT-HARVESTING COMPLEX (LHC) protein family to the thylakoid membrane (Eichacker and Henry, 2001; Schunemann, 2004). These LHC proteins have a partially conserved 18-amino acid sequence between the second and third transmembrane domains (TMDs) that was named the L18 motif (DeLille et al., 2000; Tu et al., 2000). The SRP pathway involves chloroplast (cp)SRP54, cpSRP43, cpFtsY, and the integral thylakoid membrane protein ALB3 (Li et al., 1995; Sundberg et al., 1997; Schuenemann et al., 1998; Kogata et al., 1999; for review, see Schunemann, 2004). It was shown that the L18 motif is required for interaction with cpSRP43, while cpSRP54 interacts with the hydrophobic TMDs of the LHCs and ankyrin repeat domains of cpSRP43. In light of the conserved cotranslational sorting function of the SRP pathway in bacteria and the endoplasmic reticulum, the discovery of the posttranslational SRP pathway for nucleus-encoded thylakoid proteins was surprising (for discussion, see Pool, 2005). cpSRP43 appears to be unique for organisms with LHC proteins. cpSRP54 has specific modifications that also allow it to interact with cpSRP43 and function without the SRP-RNA moiety observed in bacteria and in the cytosol of eukaryotes (Jaru-Ampornpan et al., 2007; Chandrasekar et al., 2008).

[1] This work was supported by grants from the National Science Foundation (grant nos. MCB 0343444 and MCB 0718897) and the U.S. Department of Energy (grant no. DE–FG02–04ER15560) to K.J.v.W.

[2] These authors contributed equally to the article.

[3] Present address: University of California at Los Angeles, Los Angeles, CA 90095–1569.

[4] Present address: Microdrug Development AB, 645 51 Strängnäs, Sweden.

* Corresponding author; e-mail kv35@cornell.edu.

The author responsible for distribution of materials integral to the findings presented in this article in accordance with the policy described in the Instructions for Authors (www.plantphysiol.org) is: Klaas J. van Wijk (kv35@cornell.edu).

[C] Some figures in this article are displayed in color online but in black and white in the print edition.

[W] The online version of this article contains Web-only data.

[OA] Open Access articles can be viewed online without a subscription.

www.plantphysiol.org/cgi/doi/10.1104/pp.108.124545

In contrast to posttranslational targeting, less is known about the sorting and insertion of the 40 plastid-encoded integral thylakoid membrane proteins. It is generally believed that integral thylakoid proteins are synthesized on 70S ribosomes attached to the thylakoid membrane, possibly directly docking on the SecY/E translocon. cpSRP54 also associates with 70S ribosomes (Franklin and Hoffman, 1993; Li et al., 1995; Schuenemann et al., 1998), suggesting a role for cpSRP54, but not cpSRP43, in the sorting of chloroplast-encoded proteins. Indeed, cpSRP54, but not cpSRP43, was shown to interact tightly but transiently with the first TMD of the D1 nascent chain (Nilsson et al., 1999; Nilsson and van Wijk, 2002). Moreover, during cotranslational insertion, the D1 nascent chain interacts with cpSecY (Zhang et al., 2001). In contrast, chloroplast-encoded cytochrome *f*, with cleavable lumenal transit peptide, was shown to be cotranslationally inserted into the membrane requiring cpSecA, the Sec translocon, and ATP as well as a functional LTP (Rohl and van Wijk, 2001).

cpSRP43, cpSRP54, and cpFtsY are each single copy genes in the Arabidopsis (*Arabidopsis thaliana*) genome. Homozygous single and double mutants in *cpSRP43/54* and *cpSRP54/cpFtsY* can be maintained and propagated on soil. Two mutant lines affecting cpSRP54 have been described: a dominant cosuppressor in which cpSRP54 protein levels are reduced by 70% to 93% (Pilgrim et al., 1998) and a null mutant (*ffc1-2*; Amin et al., 1999). The *ffc1-2* mutant shows both pale cotyledons and pale true leaves, in particular when plants are very young. Analysis of the Arabidopsis cpSRP43 null mutant (*chaos*; Amin et al., 1999; Klimyuk et al., 1999), cpFstY mutants (Durrett et al., 2006; Tzvetkova-Chevolleau et al., 2007), the ALB3 null mutant (Sundberg et al., 1997), and the double mutants *chaos ffc1-2* (Hutin et al., 2002) and *cpftsy ffc1-2* (Tzvetkova-Chevolleau et al., 2007) resulted in various conclusions and models. Collectively these studies showed that (1) the thylakoid protein translocon ALB3 is likely essential for LHC insertion; (2) cpSRP43 can target LHC proteins to ALB3 in the absence of cpSRP54 and cpFtsY, albeit with reduced efficiency; (3) complex formation of cpSRP54 and cpSRP43 likely prevents cpSRP43 from targeting proteins independent of cpFtsY, as evidenced by suppression of the strong *cpftsy* phenotype when crossed with *ffc1-2*; (4) the presence of cpSRP43 is not absolutely required for targeting of LHC proteins; and (5) cpSRP54, together with cpFtsY, stimulates the targeting of chloroplast-encoded thylakoid membrane proteins, but this cotranslational pathway is not essential. In disagreement with these in vivo observations, in vitro experiments indicated that cpSRP54, cpSRP43, and cpFtsY are all strictly required for targeting of LHC (Schunemann, 2004).

While the primary functions of cpSRP54 in intraplastid protein sorting are clear, little is known about the secondary effects of the loss of cpSRP54, including the plastid gene expression machinery, chaperones, and metabolic enzymes. Moreover, the SRP mutant analyses suggest alternative and compensatory pathways and factors that are so far unknown (Pilgrim et al., 1998; Amin et al., 1999; Hutin et al., 2002; Tzvetkova-Chevolleau et al., 2007). This study aims to address these aspects. To that end, we developed a mass spectrometry (MS)-based strategy for quantitative comparative proteomics of very young and mature Arabidopsis *ffc1-2* and wild-type seedlings. Isobaric stable isotope labeling (iTRAQ), isotope-coded affinity tags (ICAT), and two-dimensional gel electrophoresis (2DE) were used, since they are complementary techniques. This approach can also be applied for the analysis of other mutant seedlings (with or without developmental delays) and provides in particular an attractive general method for the analysis of chloroplast mutants, especially if these mutants have strong phenotypes from which it will be difficult to isolate significant amounts of intact chloroplasts. To further understand the chloroplast proteome homeostasis network and to follow up on the proteomics results, we generated an *ffc2-1 clpc1* double mutant. These findings are integrated in the context of chloroplast biogenesis, development, and metabolism.

RESULTS

The *ffc1-2* Mutant Is Delayed in Development Irrespective of Growth Light Intensity

The *ffc1-2* mutant was generated by ethyl methanesulfonate mutagenesis and is devoid of cpSRP54 transcript and protein (Amin et al., 1999). Throughout the remainder of this article, we refer to *ffc1-2* as *ffc*. When *ffc* was grown on agar plates under continuous moderate light (70 μmol photons m^{-2} s^{-1}), young seedlings showed yellow first leaves, which subsequently became green (Amin et al., 1999). However, when *ffc* was grown on soil with a light/dark period at 300 μmol photons m^{-2} s^{-1}, plants remained pale green with reduced rosette diameter (Hutin et al., 2002). To better characterize plant growth and development of *ffc*, wild-type and *ffc* plants were grown on soil under four different light intensities, and their visible phenotypes, rates of leaf development, and rosette diameters were carefully monitored (Fig. 1). Plants were sown directly on soil without replanting to minimize biological variation. Figure 1 shows wild-type and *ffc* plants at 33 d after planting when grown under four different light regimes (note that the magnification is not the same for each plant). *ffc* plants were always paler, with fewer leaves and a 40% to 60% reduction in rosette diameter (Fig. 1). Bolting was delayed by 25% under each light regime but occurred after formation of the same number of leaves as in the wild type, indicating that loss of cpSRP54 does result in a delay in development (data not show). Therefore, to understand the role of cpSRP54 in chloroplast and leaf development, primary cpSRP54 effects and secondary developmental effects must be distinguished.

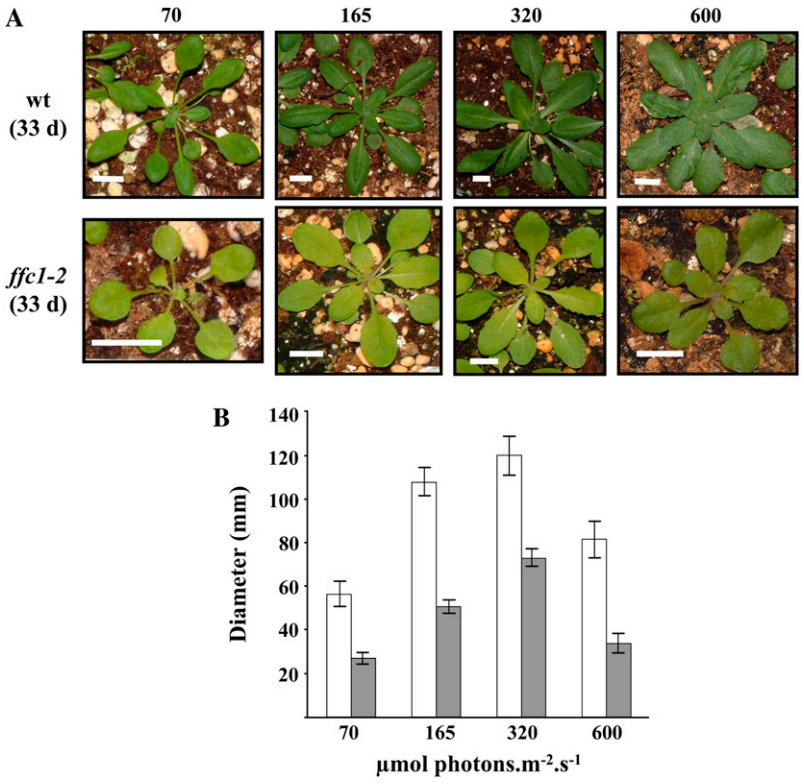

Figure 1. Growth and development of Arabidopsis (Col) wild-type and *ffc1-2* plants on soil under four different photon flux densities. A, Photos of 33-d-old plants grown under four different photon flux densities. Bars (in white) = 20 mm. B, Diameter of rosettes of 33-d-old wild-type (white) and *ffc1-2* (gray) plants grown under the different light intensities. Dim light, 70 μmol m^{-2} s^{-1}; low light, 165 μmol photons m^{-2} s^{-1}; medium light, 320 μmol photons m^{-2} s^{-1}; high light, 600 μmol photons m^{-2} s^{-1}. [See online article for color version of this figure.]

Accumulation of the cpSRP Targeting Machinery, the LHCII Family, and the D1 and D2 Proteins during Leaf Development

The chloroplast sorting machinery is particularly important during early leaf and chloroplast development, when protein synthesis and import rates are high. We postulated that the plastid protein sorting machinery might be down-regulated with progressive leaf development. There has been no systematic investigation of the response of the chloroplast sorting pathway in the *ffc* mutant. However, we note that cpSecY levels were determined in total leaf extracts of 10- and 24-d-old *ffc* and wild-type plants grown on agar plates (with vitamin mix) under continuous moderate light; this showed that cpSRP43 was not affected, while cpSecY levels were somewhat increased in *ffc* (Amin et al., 1999). In order to separate changes in protein accumulation due to the *ffc* mutation from those naturally occurring throughout development, we used the developmental stage of both wild-type and *ffc* plants, and not the age of plant material, as the basis for selecting leaf material for analysis. Developmental stages used in this study were as defined by Boyes et al. (2001). Specifically, the developmental stage of plants in the vegetative stage is determined by the number of leaves, which is indicated by the number after the digit (e.g. stage 1.4 is a young seedling with four rosette leaves of at least 1 mm). To monitor the direct effects to the protein sorting machinery along with development in both *ffc* and wild-type plants, we first determined the chlorophyll content and total protein content of the cotyledons and leaves 1/2, 3/4, 7/8, and 11/12 at developmental stages 1.4, 1.8, 1.12, and 1.16 for each leaf pair. Protein-to-chlorophyll ratios in each leaf decreased strongly (up to 50-fold) during development, reflecting assembly of the photosynthetic apparatus and accumulation of chlorophyll in the thylakoid membrane; *ffc* leaves trailed in their chlorophyll accumulation (Supplemental Fig. S1). This is consistent with a 60% reduction of chlorophyll levels observed for leaf rosettes of *ffc* plants compared with the same aged wild-type plants (Hutin et al., 2002).

Accumulation levels of the cpSRP pathway proteins cpSRP54, cpSRP43, and cpFtsY and the thylakoid protein translocons ALB3 and cpSecY/E were determined for these separate leaf pairs (Fig. 2) and cotyledons (data not shown) at different developmental plant stages. This showed that accumulation levels of SRP pathway components (cpFtsY, cpSRP43, cpSRP54, and ALB3) were strongly reduced with progressive leaf development (Fig. 2A), whereas cpSecY (Fig. 2B) and cpSecE (Fig. 2C) levels were relatively constant. Comparing *ffc* with wild-type leaves showed that, when seedlings of the same developmental stage were compared, levels of each of these sorting components were similar (except for cpSRP54, which was absent in *ffc*; Fig. 2). This provides additional evidence that comparison of wild-type and *ffc* leaves of similar development stage, rather than the same age, will best determine the direct effects of cpSRP54 deletion.

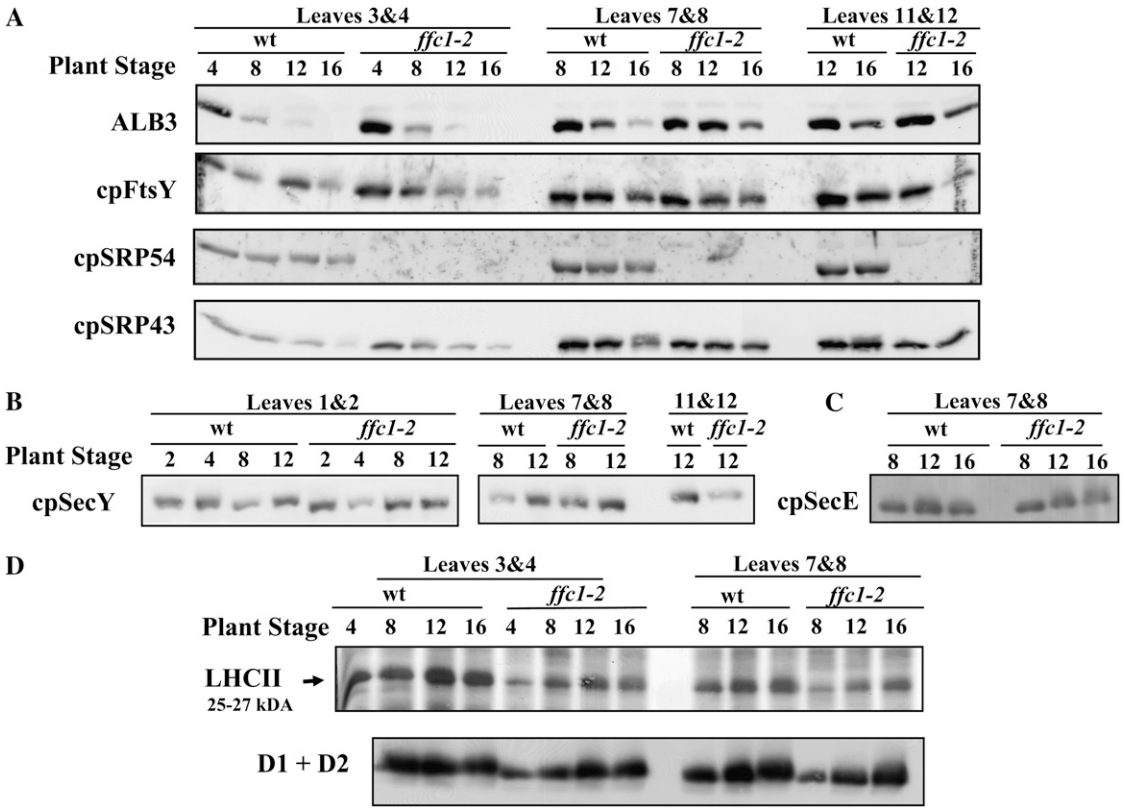

Figure 2. Analysis of chloroplast targeting components and thylakoid proteins in wild-type and *ffc1-2* during leaf development. Individual leaf pairs and plant developmental stages are indicated. A to C, Accumulation of ALB3, cpFtsY, cpSRP54, and cpSRP43 (A), cpSecY (B), and cpSecE (C) in individual leaf pairs during plant development. Protein loads were 30 μg for ALB3 and cpFtsY, 50 μg for cpSRP54, 20 μg for cpSRP43, and the membrane fraction from 100 μg of total proteins for cpSecY. D, Expression analysis of the major LHCPII, D1, and D2 proteins during leaf development in wild-type and *ffc1-2* plants. Accumulation of the LHCII family (25–27 kD) was determined by one-dimensional gels and silver staining in leaves 3/4 and 7/8 with progressive plant development. Accumulation of chloroplast-encoded thylakoid membrane proteins D1 and D2 during leaf development of leaf pairs 3/4 and 7/8 was determined by western-blot analysis. Total leaf extracts were loaded.

Silver-stained one-dimensional SDS-PAGE of whole leaf extracts of the leaf pairs at the different developmental stages showed that the overall accumulation levels of the family of major LHCII proteins (with a molecular mass of 25–27 kD) became more abundant during leaf maturation (Fig. 2D, top), as expected from previous studies. The LHCII levels were always lower in *ffc* compared with wild-type leaves. As an example, the profiles for leaves 3/4 and 7/8 at stages 1.4, 1.8, 1.12, and 1.16 are shown (Fig. 2D, top). The levels of chloroplast-encoded D1 and D2 thylakoid membrane proteins were determined by western blots (Fig. 2D, bottom). The concentrations of D1 and D2 proteins increased with leaf expansion and were initially lower in *ffc* than in the wild type. However, they reached near equivalent levels in fully expanded leaves, in contrast to LHC proteins. This is in agreement with earlier observations for whole seedlings grown of agar plates in continuous light (Pilgrim et al., 1998; Amin et al., 1999).

Comparative Proteome Analysis of Developing Seedlings of *ffc* and the Wild Type Using iTRAQ

To further determine the consequences of the loss of cpSRP54 during early stages of leaf development, total cellular leaf proteomes of *ffc* and wild-type plants were compared using iTRAQ-based protein quantification. To account for developmental delays that may mask direct effects of the loss of cpSRP54, we compared young *ffc* seedlings with an average of seven true leaves (stage 1.07) with wild-type seedlings of the same age (21 d; stage 1.11) and wild-type seedlings of the same developmental stage (stage 1.07; 17 d old; Fig. 3A). Plants at these developmental stages are shown in Figure 3B.

Total cellular leaf proteomes were extracted in the presence of SDS followed by removal of lipids and detergents in an optimized protocol for the recovery of integral membrane proteins. Each proteome was subsequently digested in solution with trypsin. A total of

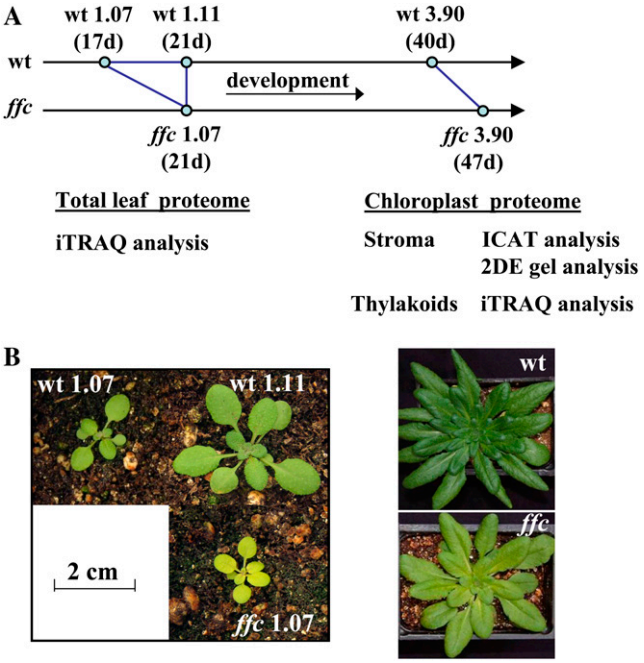

Figure 3. Mutant phenotype and developmental stage comparison. A, The developmental time line of *ffc* and wild-type plants. Plants were harvested at 17 d (wild type) and 21 d (wild type and *ffc*) for the comparison of total cellular proteomes and analyzed using the isobaric reagent iTRAQ followed by MS analysis. Stripped thylakoid membranes and soluble stroma proteins were collected from chloroplasts isolated from mature plants (40 and 47 d). The soluble stromal proteomes were analyzed using the isotopic labeling reagent ICAT followed by MS analysis and by 2DE gel analysis, while the thylakoid proteomes were compared using iTRAQ. B, Phenotype of the *ffc* mutant at 40 d with delayed development, smaller stature, and paler color. At full-grown rosette stage, the difference between *ffc* and the wild type is much less pronounced. [See online article for color version of this figure.]

30 μg of each digested proteome was labeled with the different iTRAQ reagents containing the 114-, 115-, 116-, or 117-D reporter (Supplemental Fig. S2). The labeled peptides were then mixed and separated using off-line strong cation-exchange (SCX) chromatography (Supplemental Fig. S2). Eight fractions from each SCX run were analyzed using on-line reversed-phase nanoliquid chromatography electrospray tandem mass spectrometry (LC-ESI-MS/MS). The three seedling stages (wt1.07, wt1.11, and *ffc*1.07) were directly compared within each labeling experiment, and a label switch was included to remove a possible labeling bias. These experiments were carried out with two independent biological replicates. The structure of this isobaric tagging reagent, the labeling scheme, labeling principles, and quantification are explained in Supplemental Figure S2.

A total of 123 proteins were identified unambiguously with one or more unique peptides (Supplemental Table S1A) using an established bioinformatics pipeline that included a decoy database search and a false-positive peptide identification rate of less than 1% (Zybailov et al., 2008). In addition, 39 proteins were identified as part of small gene families, in particular in the LHC family and ribosomal proteins (Supplemental Table S1A). Relevant extracted information from the MS analysis is shown in Supplemental Table S1A and can also be found in the Plant Proteomics Database (PPDB; http://ppdb.tc.cornell.edu/; see "Materials and Methods"). About 60% of the identified proteins are localized in the chloroplast, using the curated subcellular localization as described by Zybailov et al. (2008). A total of 19% of the identified proteins have at least one confirmed TMD, which is close to the predicted 22% for the whole Arabidopsis proteome (Sun et al., 2004).

The *ffc*/wild-type ratios of 97 proteins (or small families of proteins) were quantified in both biological replicates (Table I); additional proteins quantified in only one replicate are not further discussed. Details of the quantifications (e.g. individual *ffc*/wild-type ratios for each peptide sequence) can be found in Supplemental Table S2. The average coefficient of variation (CV) for the *ffc*/wild-type ratio between the biological replicates was 15%. The quantified proteome covered mostly chloroplast stromal and thylakoid proteins (30% and 39%, respectively). Quantified proteins outside the chloroplast were enriched for peroxisomal and mitochondrial proteins involved in photorespiration as well as for cytosolic proteins involved in protein synthesis (Table I). The *ffc*/wild-type ratios that are below 0.85 or above 1.15 and are also 2 SD away from unity are marked in boldface (Table II). This corresponds to $P < 0.05$, assuming normal distribution.

Differences between the Two Developmental Stages in Wild-Type Plants Determined by iTRAQ

When comparing the two wild-type seedling developmental stages, it is notable that levels of major LHCI and LHCII antennae proteins in the thylakoid proteome increase up to 50% during these 4 d of plant growth, reflecting the buildup of the photosynthetic apparatus during leaf development. This also underlines the importance of accounting for a developmental delay when addressing the role of cpSRP54 and biogenesis of the LHC family. Interestingly, accumulation of the subunits of PSI and PSII core complexes and the thylakoid ATP synthase complex increased on average only by 9%, 5%, and 5%, respectively, indicating that assembly of the peripheral antennae complexes trails the accumulation of the PSI and PSII cores as well as ATP synthase. Levels of 12 quantified Calvin cycle enzymes, and most other quantified functions inside and outside of the chloroplast, did not change between stages 1.07 and 1.14 in wild-type seedlings (Table I). We note that the *ffc*/wild-type ratios within these complexes and pathways were highly consistent, providing additional testimony for the accuracy and significance of the quantitative analysis.

Table I. *Quantified proteins in seedlings using iTRAQ with two biological replicates between wt1.07/wt1.11 and ffc1.07/wt1.07 and ffc1.07/wt1.11*

Protein Name	Accession[a]	wt1.07/wt1.11[b]	*ffc*1.07/wt1.07[b]	*ffc*1.07/wt1.11[b]	Location	Function
LHCII-1.1, -1.2, -1.3, -1.5	AT1G29910.1 AT1G29920.1 AT1G29930.1 AT2G34420.1	**0.80 ± 0.04**	**0.73 ± 0.08**	**0.59 ± 0.10**	Thylakoid, integral	PSII antennae
LHCII-1.4	*AT2G34430.1*	0.70 ± 0.07	0.70 ± 0.33	0.50 ± 0.28	Thylakoid, integral	PSII antennae
LHCII-2.1, -2.2	AT2G05100.1 AT2G05070.1	0.97 ± 0.00 0.95	**0.80 ± 0.09** 0.76	**0.74 ± 0.08** 0.71	Thylakoid, integral	PSII antennae
LHCII-3[c]	AT5G54270.1				Thylakoid, integral	PSII antennae
LHCII-4.1 (CP29)	AT5G01530.1	0.85 ± 0.10	0.85 ± 0.29	**0.78 ± 0.07**	Thylakoid, integral	PSII antennae
LHCII-4.2 (CP29)	AT3G08940.2	0.84 ± 0.14	0.83 ± 0.02	0.68 ± 0.07	Thylakoid, integral	PSII antennae
LHCII-5 (CP26)	AT4G10340.1	**0.85 ± 0.04**	1.01 ± 0.04	0.92 ± 0.03	Thylakoid, integral	PSII antennae
LHCII-6 (CP24)	AT1G15820.1	**0.82 ± 0.08**	0.85 ± 0.04	**0.74 ± 0.11**	Thylakoid, integral	PSII antennae
LHCI-1.1 (LHCI-730)	AT3G54890.1	0.75 ± 0.22	0.88 ± 0.16	**0.79 ± 0.12**	Thylakoid, integral	PSI antennae
LHCI-3 (LHCI-680A)	AT1G61520.1	**0.58 ± 0.22**	1.07 ± 0.71	0.74 ± 0.22	Thylakoid, integral	PSI antennae
LHCI-4 (LHCI-730)	AT3G47470.1	**0.68 ± 0.09**	**0.78 ± 0.02**	**0.58 ± 0.00**	Thylakoid, integral	PSI antennae
PsbA D1	ATCG00020.1	0.99 ± 0.17	0.92 ± 0.14	0.91 ± 0.26	Thylakoid, integral	PSII core
PsbD D2	ATCG00270.1	**0.88 ± 0.02**	**0.85 ± 0.04**	**0.74 ± 0.04**	Thylakoid, integral	PSII core
PsbB CP47	ATCG00680.1	0.90 ± 0.10	0.90 ± 0.14	**0.76 ± 0.15**	Thylakoid, integral	PSII core
PsbC CP43	ATCG00280.1	0.91 ± 0.03	**0.84 ± 0.06**	**0.75 ± 0.06**	Thylakoid, integral	PSII core
PsbE cytochrome b559α	ATCG00580.1	0.99 ± 0.25	1.08 ± 0.11	1.06 ± 0.17	Thylakoid, integral	PSII core
PsbR	AT1G79040.1	1.07 ± 0.02	0.87 ± 0.08	0.93 ± 0.11	Thylakoid, integral	PSII core
PsbS	AT1G44575.1	1.10 ± 0.15	**1.39 ± 0.11**	1.56 ± 0.31	Thylakoid, integral	PSII antennae quencher
PsbO OEC33 and OEC-like	AT3G50820.1 AT5G66570.1	0.92 ± 0.07	0.99 ± 0.00	**0.83 ± 0.07**	Thylakoid, lumenal side	PSII OEC
PsbP OEC23 family	*AT2G30790.1* AT1G06680.1	0.87 ± 0.12	0.91 ± 0.16	**0.78 ± 0.02**	Thylakoid, lumenal side	PSII OEC
PsbQ OEC16 Tat ltp	AT4G21280.1	0.95 ± 0.08	1.26 ± 0.03	1.13 ± 0.14	Thylakoid, lumenal side	PSII OEC
PsbQ OEC16-like Tat lTP	AT4G05180.1	0.87 ± 0.09	**0.68 ± 0.10**	**0.52 ± 0.06**	Thylakoid, lumenal side	PSII OEC
PetA - cytochrome *f*	ATCG00540.1	0.93 ± 0.22	0.92 ± 0.10	0.92 ± 0.21	Thylakoid, integral	Cytochrome b_6/f
PetC - Rieske iron-sulfur protein	AT4G03280.1	**0.77 ± 0.06**	1.31 ± 0.28	1.00 ± 0.14	Thylakoid, lumenal side	Cytochrome b_6/f
Plastocyanin-1 (PC-1)	AT1G20340.1	2.54 ± 0.96	**0.58 ± 0.08**	1.50 ± 0.74	Thylakoid, lumenal side	Lumenal electron carrier
FNR-1	AT5G66190.1	0.93 ± 0.21	1.07 ± 0.06	**0.88 ± 0.02**	Thylakoid, stromal side	Ferredoxin reductase
PsaA subunit Ia	ATCG00350.1	0.95 ± 0.05	**0.73 ± 0.03**	**0.70 ± 0.02**	Thylakoid, integral	PSI core
PsaB subunit Ib	ATCG00340.1	**0.86 ± 0.05**	**0.53 ± 0.11**	**0.48 ± 0.13**	Thylakoid, integral	PSI core
PsaD-1, -2 subunit II	AT4G02770.1 AT1G03130.1	1.06 ± 0.19	**0.64 ± 0.18**	**0.67 ± 0.10**	Thylakoid, stromal side	PSI core
PsaF subunit III	AT1G31330.1	**0.86 ± 0.06**	**0.63 ± 0.01**	**0.54 ± 0.05**	Thylakoid, integral	PSI core
PsaG subunit V	AT1G55670.1	0.87 ± 0.17	**0.74 ± 0.05**	**0.65 ± 0.17**	Thylakoid, integral	PSI core
CF1a - atpA	ATCG00120.1	0.99 ± 0.03	**0.85 ± 0.06**	**0.86 ± 0.00**	Thylakoid, stromal side	ATP synthase
CF1b - atpB	ATCG00480.1	0.99 ± 0.10	**0.84 ± 0.03**	**0.82 ± 0.02**	Thylakoid, stromal side	ATP synthase
CF1y - atpC	AT4G04640.1	0.89 ± 0.08	1.00 ± 0.02	**0.73 ± 0.00**	Thylakoid, stromal side	ATP synthase
CF1d - atpD	AT4G09650.1	0.90 ± 0.00	**0.83 ± 0.01**	**0.77 ± 0.07**	Thylakoid, stromal side	ATP synthase
CF1e - atpE	ATCG00470.1	0.90 ± 0.07	0.85 ± 0.10	0.91 ± 0.05	Thylakoid, stromal side	ATP synthase
CFO-II - atpG	AT4G32260.1	1.07 ± 0.07	1.10 ± 0.15	1.18 ± 0.08	Thylakoid, integral	ATP synthase
ATP synthase α mitochondrial	AT2G07698.1	**0.81 ± 0.03**	**1.33 ± 0.06**	1.08 ± 0.01	Mitochondria	ATP synthesis
ATP synthase β mitochondrial	AT5G08670.1 AT5G08680.1 AT5G08690.1	1.19 ± 0.10	0.96 ± 0.14	1.01 ± 0.04	Mitochondria	ATP synthesis
Fru-bisphosphate aldolase-1 (SFBA-1)	AT2G21330.1	1.12 ± 0.06	**1.41 ± 0.04**	**1.53 ± 0.01**	Plastid stroma; plastoglobules	Calvin cycle
Fru-bisphosphate aldolase-2 (SFBA-2)	AT4G38970.1	0.85 ± 0.13	**1.54 ± 0.01**	**1.41 ± 0.11**	Plastid stroma; plastoglobules	Calvin cycle
Phosphoribulokinase-2 (PRK-2)	AT1G32060.1	0.98 ± 0.11	1.16 ± 0.19	1.26 ± 0.02	Plastid stroma	Calvin cycle
Rubisco activase	AT2G39730.1	1.05 ± 0.07	1.25 ± 0.09	**1.38 ± 0.14**	Plastid stroma	Calvin cycle
Rubisco large subunit (RBCL)	ATCG00490.1	1.06 ± 0.05	**0.90 ± 0.06**	0.96 ± 0.01	Plastid stroma	Calvin cycle

(*Table continues on following page.*)

Table I. (*Continued from previous page.*)

Protein Name	Accession[a]	wt1.07/wt1.11[b]	*ffc*1.07/wt1.07[b]	*ffc*1.07/wt1.11[b]	Location	Function
Rubisco small subunit 1b (RBCS-1b)	AT5G38410.1 AT5G38420.1 AT5G38430.1	1.13 ± 0.31	0.93 ± 0.02	1.01 ± 0.15	Plastid stroma	Calvin cycle
Rubisco small subunit 4 (RBCS-4)	AT1G67090.1	1.05 ± 0.04	**0.94 ± 0.02**	0.98 ± 0.00	Plastid stroma	Calvin cycle
Sedoheptulose-bisphosphatase (SBPase)	AT3G55800.1	1.10 ± 0.06	1.26 ± 0.06	**1.44 ± 0.05**	Plastid stroma	Calvin cycle
Glyceraldehyde-3-P dehydrogenase A-1, A-2, B	AT1G12900.1 AT3G26650.1 AT1G42970.1	1.00 ± 0.02	**1.43 ± 0.04**	**1.44 ± 0.06**	Plastid stroma	Calvin cycle; glycolysis
Phosphoglycerate kinase-1 (PGK-1)	AT3G12780.1	1.00 ± 0.06	**1.47 ± 0.10**	**1.40 ± 0.04**	Plastid stroma	Calvin cycle; glycolysis
Transketolase-1 (TKL-1)	AT3G60750.1	1.21 ± 0.00	**1.38 ± 0.15**	**1.52 ± 0.18**	Plastid stroma	Calvin cycle; OPP
Transketolase-2 (TKL-2)	AT2G45290.1	1.12 ± 0.29	1.54 ± 0.57	**1.63 ± 0.20**	Plastid stroma	Calvin cycle; OPP
TPT - IEP30 = phosphate/triose-P translocator	AT5G46110.1	1.12 ± 0.05	**1.44 ± 0.05**	**1.63 ± 0.04**	Inner envelope, integral	Plastid envelope transport
Glyceraldehyde-3-P dehydrogenase C-1 (GapC-1)	AT3G04120.1	1.15 ± 0.05	1.04 ± 0.05	1.18 ± 0.10	Cytosol	Glycolysis
Ala 2-oxoglutarate aminotransferase 1 (GGAT1)	AT1G23310.1	0.97 ± 0.30	0.93 ± 0.42	0.98 ± 0.70	Peroxisome	Photorespiration
Gly decarboxylase P protein (Atgldp)	*AT2G26080.1* *AT4G33010.1*	**1.34 ± 0.07**	**1.61 ± 0.07**	**2.18 ± 0.19**	Mitochondria	Photorespiration
Gly decarboxylase T protein	AT1G11860.1	1.15 ± 0.29	1.00 ± 0.07	1.12 ± 0.18	Mitochondria	Photorespiration
Gly/Ser hydroxymethyltransferase (SHM1)	AT4G37930.1	1.19 ± 0.21	**1.30 ± 0.13**	**1.73 ± 0.15**	Mitochondria	Photorespiration
Glycolate oxidase-1 (GOX-1)	AT3G14415.1	1.27 ± 0.47	**1.30 ± 0.15**	1.84 ± 0.60	Peroxisome	Photorespiration
Glycolate oxidase-2 (GOX-2)	AT3G14420.1	1.13 ± 0.17	**1.47 ± 0.19**	**1.87 ± 0.20**	Peroxisome	Photorespiration
Gln synthase (GS2)	AT5G35630.1	1.00 ± 0.06	1.14 ± 0.28	1.00 ± 0.03	Plastid stroma	Photorespiration; nitrogen metabolism
Catalase 2 and 3 (CAT2, -3)	*AT1G20620.1* AT4G35090.1	0.97 ± 0.19	**1.45 ± 0.14**	**1.39 ± 0.14**	Peroxisome	Photorespiration; ROS defense
S-Adenosyl-L-homo-Cys hydrolase (HOG1)	AT4G13940.1	**0.74 ± 0.017**	**1.35 ± 0.08**	0.98 ± 0.11	Cytosol	SAM cycle
5-Methyltetrahydropteroyltriglutamate-homo-Cys *S*-methyltransferase	AT5G17920.1	1.07 ± 0.09	1.15 ± 0.11	1.19 ± 0.01	Cytosol	SAM cycle
SAM synthetase 3 (MTO3)	AT3G17390.1	1.03 ± 0.11	0.96 ± 0.02	0.99 ± 0.09	Cytosol	SAM cycle
cpHSP70-1, -2	AT4G24280.1 AT5G49910.1	1.27 ± 0.45	**1.81 ± 0.29**	**2.07 ± 0.18**	Plastid stroma	Protein folding
Cpn21 (also Cpn20)	AT5G20720.1	1.25 ± 0.05	1.18 ± 0.15	**1.46 ± 0.05**	Plastid stroma	Protein folding
Cpn60-α-1	AT2G28000.1	1.07 ± 0.03	**1.89 ± 0.02**	**2.00 ± 0.19**	Plastid stroma	Protein folding
Cpn60-β-2	AT1G55490.1	1.02 ± 0.02	**1.40 ± 0.03**	**1.50 ± 0.12**	Plastid stroma	Protein folding
Peptidylprolyl isomerase ROC4	AT3G62030.1	1.16 ± 0.08	**1.49 ± 0.03**	**1.81 ± 0.16**	Plastid stroma	Protein folding
30S ribosomal protein S1	AT5G30510.1	1.08 ± 0.13	1.03 ± 0.17	1.12 ± 0.31	Plastid stroma	Plastid ribosome
50S ribosomal protein L12-A, -C	AT3G27850.1 AT3G27830.1	1.08 ± 0.28	1.30 ± 0.22	1.49 ± 0.27	Plastid stroma	Plastid ribosome
Elongation factor Tu (EF-Tu1), plastid	AT4G20360.1	1.07 ± 0.08	**1.51 ± 0.18**	**1.55 ± 0.21**	Plastid stroma	Protein synthesis
Rap38 or CSP41B	AT1G09340.1	0.85 ± 0.14	**1.37 ± 0.11**	1.02 ± 0.04	Plastid stroma; plastoglobules	RNA binding
RNA-binding protein CP29 A′	AT3G53460.1	1.42 ± 0.25	1.33 ± 0.52	1.96 ± 1.07	Plastid stroma	RNA binding
RNA-binding protein CP29 B′	AT2G37220.1	1.07 ± 0.17	**1.62 ± 0.17**	**1.70 ± 0.10**	Plastid stroma	RNA binding
RNA-binding protein CP31	AT4G24770.1	1.23 ± 0.08	**1.53 ± 0.07**	2.14 ± 0.60	Plastid stroma	RNA binding
ClpC1,2 (also named HSP93-III and -V)	AT3G48870.1 AT5G50920.1	1.00 ± 0.03	1.67 ± 0.56	1.67 ± 0.37	Plastid stroma/inner envelope	Protein degradation
FtsH1, -5	*AT1G50250.1* *AT5G42270.1*	0.92 ± 0.37	**1.69 ± 0.07**	1.54 ± 0.72	Thylakoid, integral	Protein degradation
HSP70 family (cytosol)	*AT1G16030.1* AT3G12580.1 *AT3G09440.1* *AT5G02490.1* AT5G02500.1	**0.82 ± 0.07**	**1.46 ± 0.08**	1.50 ± 0.38	Cytosol	Protein folding
40S ribosomal protein S14	AT3G11510.1	**0.85 ± 0.01**	1.35 ± 0.30	1.14 ± 0.24	Cytosol	Cytosolic ribosome
40S ribosomal protein S4 A, B, D	AT2G17360.1 AT5G07090.1 AT5G58420.1	1.15 ± 0.39	**1.28 ± 0.07**	1.29 ± 0.18	Cytosol	Cytosolic ribosome
40S ribosomal protein S9	AT5G15200.1	0.92 ± 0.00	**1.32 ± 0.04**	1.12 ± 0.12	Cytosol	Cytosolic ribosome
60S acidic ribosomal protein P2	AT2G27720.1	1.06 ± 0.09	1.18 ± 0.19	1.11 ± 0.06	Cytosol	Cytosolic ribosome
60S ribosomal protein L10 A, B, C	*AT1G14320.1* AT1G26910.1 *AT1G66580.1*	1.21 ± 0.63	1.08 ± 0.03	1.30 ± 0.65	Cytosol	Cytosolic ribosome

(*Table continues on following page.*)

Table I. (*Continued from previous page.*)

Protein Name	Accession[a]	wt1.07/wt1.11[b]	*ffc*1.07/wt1.07[b]	*ffc*1.07/wt1.11[b]	Location	Function
Elongation factor 1-α family (EF-Tu)	AT1G07920.1 AT1G07930.1 AT1G07940.1 AT5G60390.1	1.11 ± 0.07	1.27 ± 0.14	1.44 ± 0.22	Cytosol	Protein synthesis
Elongation factor 2 (EF-2)	AT1G56070.1	1.12 ± 0.04	1.07 ± 0.26	1.08 ± 0.51	Cytosol	Protein synthesis
Expressed protein; weak similarity to 60S ribosomal su	AT1G13930.1	**0.82 ± 0.01**	1.29 ± 0.57	**1.41 ± 0.05**	Cytosol	Protein synthesis
UBQ8 (ubiquitin 8)	*AT5G37640.1* AT3G09790.1	0.86 ± 0.21	1.14 ± 0.26	0.96 ± 0.01	Cytosol/nucleus	Protein degradation
Glutathione transferase (Tau class) - ATGSTU20	AT1G78370.1	1.23 ± 0.08	0.82 ± 0.15	0.99 ± 0.22	Not plastid	Redox
Peroxiredoxin IIE (PrxII E)	AT3G52960.1	1.42 ± 0.43	**1.33 ± 0.12**	1.91 ± 0.75	Plastid stroma	Redox
Gly-rich RNA-binding protein 7, 8	AT2G21660.2 AT4G39260.1	1.15 ± 0.11	1.32 ± 0.28	**1.49 ± 0.18**	Not plastid	RNA binding
Malate dehydrogenase (PMDH2)	AT5G09660.1	**0.67 ± 0.04**	**1.38 ± 0.33**	1.07 ± 0.05	Peroxisome	Gluconeogenesis
Thioglucoside glucohydrolase 1, 2 (TGG1, -2) (myrosinase)	*AT5G25980.1* *AT5G26000.1*	0.64 ± 0.31	0.82 ± 0.19	**0.49 ± 0.13**	Not plastid	Secondary metabolism
Lipoxygenase AtLOX2, plastid	AT3G45140.1	0.90 ± 0.08	**0.84 ± 0.14**	**0.71 ± 0.13**	Plastid stroma	Jasmonate synthesis
β-Carbonic anhydrase 2 (CA2)	AT5G14740.2	1.28 ± 0.02	1.15 ± 0.12	**1.36 ± 0.02**	Plastid stroma	Organic transformation
β-Carbonic anhydrase 1 (βCA1)	AT3G01500.1	0.99 ± 0.11	1.14 ± 0.07	1.06 ± 0.01	Plastid stroma	Organic transformation
Tubulin α-2, -3, -4, -5, -6 chain	AT1G04820.1 AT1G50010.1 AT4G14960.1 AT5G19770.1 AT5G19780.1	0.90 ± 0.23	1.12 ± 0.39	0.96 ± 0.10	Not plastid	Cell organization
14-3-3 proteins GF14 χ, ω, ϕ (grfCP1, -2, -4)	*AT1G35160.1* AT4G09000.1 *AT1G78300.1*	0.92 ± 0.20	1.30 ± 0.29	1.22 ± 0.50	Multiple?	Signaling

[a]Underlined if the accession was quantified with only shared peptides; italic if the accession did not pass the strict filter for identification, but a subset of the peptides used for quantification do match this isoform. [b]Average ratios with SD. Numbers in boldface are up-regulated or down-regulated and at least 2 SD away from unity. [c]Present in only one biological replicate; in this table for completeness.

Differential Protein Accumulation between *ffc* and Wild-Type Seedlings Determined by iTRAQ

LHCI and LHCII Proteins and PsbS

There are 22 LHC proteins in the antennae of PSI and PSII, and they are arranged in six LHCII and five LHCI subfamilies (Fig. 4). They contain a partially conserved L18 hydrophilic domain located between TMDs 2 and 3 (Fig. 4); this L18 domain was shown to be essential for interaction with cpSRP43 and formation of the ''transit complex'' (DeLille et al., 2000; Tu et al., 2000). We detected and quantified nine out of the 11 LHC subfamilies; their accumulation levels in *ffc* were between 70% and 100% of wt1.07 levels. When comparing LHC levels in *ffc*1.07 and wt1.11, these accumulation levels were further reduced as a consequence of the developmental delay (Table I). Compared with other LHC members, the LHCII-1 family was most reduced, while CP26 (LHCII-6) was unaffected. The abundant PsbS protein with pigment-binding domains and four TMDs (rather than three in the LHC family) accumulated at 40% higher levels in *ffc* than in the wild type, in agreement with observations that PsbS does not require the SRP pathway in vivo (Tzvetkova-Chevolleau et al., 2007) and can stably accumulate in the thylakoid, independent of PSII (Niyogi et al., 2005).

Photosynthetic Thylakoid Complexes

The four major complexes, PSII, PSI, the ATP synthase, and the cytochrome b_6f complex, contain several chloroplast-encoded integral membrane proteins that are potential substrates of the cpSRP54-dependent cotranslational insertion pathway. The accumulation levels of these chloroplast-encoded proteins could be directly affected by the lack of cpSRP54 in the *ffc* mutant. The nucleus-encoded subunits in these complexes are not known to require the cpSRP pathway.

Within the PSII core complex, 11 proteins were quantified (Table I), including five chloroplast-encoded proteins (D1, D2, CP43, CP47, and cytochrome *b559*α), the nucleus-encoded integral membrane core protein PsbR, and the three nucleus-encoded proteins of the water-splitting complex (OEC16, OEC23, and OEC33 and some of their homologues). The average accumulation of PSII core proteins in *ffc* was 8% reduced when compared with wt1.07 and 19% reduced when compared with wt1.11. The Sec-dependent OEC33 and the TAT-dependent OEC23 were unaffected in *ffc*, while the two TAT-dependent OEC16 homologues showed a strong differential response, suggesting that they have complementary functions (Table I). Five PSI core subunits were quantified: the major PSI core subunits PsaA and PsaB (chloroplast encoded), and PsaD, PsaF, and PsaG (nucleus encoded). An average reduction of

Table II. *Comparative analysis of soluble stromal proteins from isolated chloroplasts of fully developed leaf rosettes of ffc and wt plants using ICAT*

Protein Name[a]	Gene Identifier[b]	*ffc*/wt (Experiment 1 + 2)[c]	SD[d]	CV[e]	Function
FNR-2	At1g20020.1	0.98	0.06	5.6	PS light reaction
2-Phosphoglycolate phosphatase 1, 2 (PGP-1, -2)	At5g36700.1 At5g36790.1	0.94	0.04	4.3	Photorespiration
Rubisco large subunit (RBCL)	AtCg00490	**0.89**	0.02	2.3	Calvin cycle
Ribulose-5-P 3-epimerase (RPE)	At5g61410.1	0.92	0.12	13.1	Calvin cycle
Phosphoribulokinase-2 (PRK-2)	At1g32060.1	**0.85**	0.04	4.9	Calvin cycle
Rubisco activase	At2g39730.1	**0.87**	0.04	5.1	Calvin cycle
Rubisco small subunit family (RBCS-1, -2, -3b, -4)	At5g38410.1 At5g38420.1 At5g38430.1 At1g67090.1	0.80	0.17	21.5	Calvin cycle
Glyceraldehyde-3-P dehydrogenase B (GAPB)	At1g42970.1	**0.56**	0.19	34.7	Calvin cycle
Glyceraldehyde-3-P dehydrogenase A-1, -2 (GAPA-1, -2)	At1g12900.1 At3g26650.1	**0.62**	0.17	27.1	Calvin cycle
Triosephosphate isomerase-1 (TPI-1)	At2g21170.1	**0.71**	0.01	1.1	Calvin cycle
Fru-bisphosphate aldolase-2 (SFBA-2)	At4g38970.1	0.80	0.28	35.4	Calvin cycle
Fru-bisphosphatase-1 (FBPA)	At3g54050.1	0.84	0.27	31.7	Calvin cycle
Sedoheptulose-bisphosphatase (SBPase)	At3g55800.1	0.74	0.29	38.5	Calvin cycle
Transketolase-1, -2 (TKL-1, -2)	At3g60750.1 At2g45290.1	0.76	0.16	21.296	Calvin cycle
Starch phosphorylase-1	At3g29320.1	1.20	0.27	22.5	Starch phosphorylase
Haloacid dehalogenase-like hydrolase-2	At3g48420.1	0.97	0.00	0.3	Carbohydrate metabolism
Haloacid dehalogenase-like hydrolase-3	At4g39970.1	1.27	0.34	26.4	Carbohydrate metabolism
Aldo/keto reductase family	At2g27680.1	0.97	0.00	0.0	Carbohydrate metabolism
Aldose 1-epimerase	At5g66530.1	0.89	0.06	6.9	Pentose phosphate pathway?
Putative (plastid) phosphofructokinase	At1g66430.1	0.69	0.19	28.0	Pentose phosphate pathway?
Epimerase/dehydratase	At2g37660.1	0.98	0.05	5.0	Pentose phosphate pathway?
Malate dehydrogenase (NAD)	At3g47520.1	0.76	0.18	23.9	Organic transformation
β-Carbonic anhydrase-1 (β-CA1)	At3g01500.1	0.60	0.23	38.0	Carbonic anhydrases
Acyl-[acyl-carrier-protein] desaturase-1	At2g43710.1	0.86	0.12	14.5	Fatty acid synthesis and elongation
Ferredoxin-dependent glutamate synthase/glu1/Fd-GOGAT 1	At5g04140.1	0.84	0.08	9.9	Nitrogen metabolism
Sulfite reductase	At5g04590.1	1.13	0.18	16.0	Sulfur/Cys metabolism
Cys synthase 1 (OAS-B)	At2g43750.1	**0.62**	0.05	8.7	Cys metabolism
Glyoxalase I-1, putative (lactoylglutathione lyase)	At1g67280.1	0.99	0.03	3.0	Amino acid metabolism
Lipoxygenase AtLOX2	At3g45140.1	0.89	0.17	19.6	Jasmonate synthesis
Hydroxymethylbilane synthase (HEMC)	At5g08280.1	0.91	0.11	12.3	Tetrapyrrole synthesis
Uroporphyrinogen decarboxylase (UPD)	At2g40490.1	1.04	0.07	6.3	Tetrapyrrole synthesis
Glutathione peroxidase 2 (GPX2)	At2g25080.1	0.98	0.10	9.8	ROS defense
L-Ascorbate peroxidase, stromal (sAPX)	At4g08390.1	**1.56**	0.07	4.4	ROS defense
Peroxiredoxin IIE (PrxII E)	At3g52960.1	**0.89**	0.04	4.3	Redox regulation
Oxidoreductase NAD-binding domain-containing protein	At1g15140.1	0.86	0.10	11.3	Miscellaneous oxidases
Rap38 or CSP41B	At1g09340.1	0.95	0.13	14.0	RNA binding
30S rps2 ribosomal protein S2	AtCg00160	1.03	0.04	4.0	Protein synthesis
Elongation factor Tu-G (EF-G) (sco1)	At1g62750.1	0.88	0.19	21.3	Protein synthesis
ClpC1/ClpC2	At5g50920.1 At3g48870.1	1.01	0.08	7.6	Protein degradation
AtPrep1 - (AtZnMP) metalloprotease dually targeted	At3g19170.1	0.93	0.08	8.7	Protein degradation
cpHSP70-1 (DnaK homologue)[f]	At4g24280.1	0.93	0.14	15.3	Protein folding
cpHSP70-2 (Dnak homologue)[f]	At5g49910.1	0.95	0.29	30.9	Protein folding
Peptidylprolyl isomerase ROC4	At3g62030.1	0.94	0.09	10.0	Protein folding
Cpn60-β-2[g] (partial overlap with Cpn60-β-1 and -3)	At1g55490.1	1.06	0.15	14.3	Protein folding
Unknown function	At5g45170.1	**0.63**	0.09	14.6	No assigned function
Unknown function	At1g16080.1	1.07	0.04	3.7	No assigned function

[a]Down-regulated or up-regulated proteins are marked in boldface (at least 2 SD away from unity). [b]Some ICAT-labeled peptides matched to one or more close homologues (e.g. PGP-1, -2, and the RBCS family); these homologues are listed. [c]Ratios of down-regulated or up-regulated proteins are marked in boldface (at least 2 SD away from unity). [d]SD of the average values. [e]Coefficient of variation of the averages in percentage. [f]Partial overlapping peptides. [g]Partial overlap with Cpn60-β-1 and -3 (At3g13470 and At5g56500).

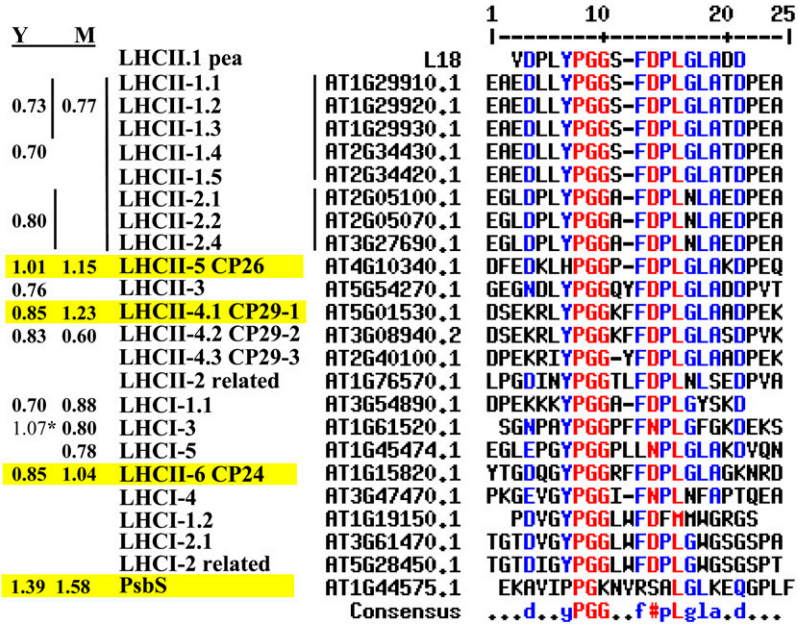

Figure 4. Alignment of the L18 motif from pea (*Pisum sativum*) Lhcb1 and all 22 Arabidopsis LHC proteins as well as PbsS. *ffc*/wild-type ratios for young seedlings (stage 1.07) and for fully developed rosette leaves (M) as determined by iTRAQ analysis are indicated. M, Mature plants; Y, young seedlings. The asterisk indicates that this ratio has a very high CV.

54% for these PSI core subunits was observed when comparing *ffc* with wt1.07, which increased to 65% when comparing *ffc* with wt1.11. When comparing the changes in accumulation for the core subunits of these two photosystems, it is clear that the PSI/PSII ratio is lower in *ffc* as compared with the wild type. The PSI/PSII ratio (calculated from the average *ffc*/wild-type ratio of the core subunits) does not change during the 4 d of development in the wild type (wt1.07/wt1.11 = 0.98) but is only about 70% of the wild-type ratio in *ffc* seedlings (0.70 for *ffc*/wt1.07 and 0.67 for *ffc*/wt1.11).

Three chloroplast-encoded (CF1α, -β, and -ε) and two nucleus-encoded peripheral (CF1δ and -γ) ATP synthase subunits, as well as one nucleus-encoded integral ATP synthase subunit (CF0-II), were quantified. The peripheral subunits of this complex were reduced by 15% in *ffc* as compared with wt1.07 and by 22% compared with wt1.11, while CF0-II was unaffected in *ffc*. In vitro studies suggested that the CF0-II protein inserts "spontaneously" into the membrane (Michl et al., 1994), which is consistent with our observations.

Chloroplast Protein Synthesis and Homeostasis

Stromal chaperones (Cpn60, Cpn21, and Hsp70) involved in protein folding and maturation, as well as a highly abundant protein isomerase without known function (ROC4), increased 40% to 89% in *ffc* as compared with wt1.07 (Table I). The increase was slightly higher (46%–107%) when compared with wt1.11. ClpC1 and -2 levels increased 67% in the *ffc* mutant compared with both wt1.07 and wt1.11. ClpC1 and -2 are members of the Hsp100 family; in particular, ClpC1 has been shown to be involved in protein import (Kovacheva et al., 2007). ClpC1 and -2 are likely also involved in the delivery of proteins for degradation to the stromal ClpPR protease complex (Adam et al., 2006). Three abundant RNA-binding proteins (CP29A, CP29B, and CP31) involved in mRNA stability and the elongation factor and chaperone EF-Tu1 (Rao et al., 2004) accumulated to 50% higher levels in *ffc*. The thylakoid membrane proteases FtsH1 and -5 accumulated to 69% higher levels in *ffc* compared with the wild type, suggesting an increased need for degradation within the thylakoid membrane.

Calvin Cycle, Photorespiration, and Nitrogen Assimilation

The small and large subunits of Rubisco accumulated at slightly lower levels in *ffc* (Table I). In contrast, nine other Calvin Cycle enzymes accumulated on average at 38% (±13%) higher levels in *ffc* compared with wt1.07 (and 45% ± 11% compared with wt1.11). Eight peroxisomal and mitochondrial proteins involved in various aspects of photorespiration were quantified. Glycolate oxidases 1 and 2, the first respiratory enzymes in the peroxisomes, increased by 39% in *ffc* as compared with wt1.07 (and 86% compared with wt1.11). Consistently, catalases 2 and 3, involved in the detoxification of hydrogen peroxide released by glycolate oxidases, increased 45% in *ffc*. Three mitochondrial photorespiratory enzymes were quantified. The P protein of the Gly decarboxylase complex increased by 61% ± 7% in *ffc* when compared with wt1.07 (and 118% ± 19% when compared with wt1.11), while the T subunit was unaffected. The enzyme immediately downstream of Gly decarboxylase, Gly/Ser hydroxymethyltransferase, increased by 61% ± 7% in *ffc* when compared with wt1.07 (118% ± 19% compared with wt1.11). Chloroplast stromal Glu synthase, involved

in the photorespiratory cycle as well as nitrogen assimilation, was not significantly affected in *ffc*.

Cytosolic Functions

Nine cytosolic proteins involved in protein synthesis and folding were quantified (Table I). However, several peptides used for these quantifications matched multiple members of the respective protein families, reducing the value of the quantification. Nevertheless, it appears that cytosolic protein homeostasis was not or only slightly affected (*ffc*/wild type = 1.27 ± 0.13). Three enzymes of the cytosolic *S*-adenosyl-Met (SAM) cycle were quantified but did not show any consistent change in *ffc*.

Overview of Comparative Analysis of the *ffc* and Wild-Type Chloroplast Proteome from Mature Leaf Rosettes

To compare the mature chloroplast proteomes of wild-type and *ffc* plants, chloroplasts were isolated from fully grown rosettes prior to bolting from 40-d-old wild-type plants and 47-d-old *ffc* plants, both at growth stage 3.90, as defined by Boyes et al. (2001; Fig. 3, A and B). The isolated chloroplasts were fractionated into soluble stroma and thylakoid membranes. The isolated thylakoid membranes were stripped of lumenal and peripheral proteins, and the remaining membrane proteomes of *ffc* and the wild type were compared using iTRAQ labeling and quantification by MS/MS analysis (see Supplemental Fig. S2 for experimental design). The stromal proteomes of wild-type and *ffc* plants were compared using differential stable isotope labeling with cleavable ICAT (Fig. 5; Tao and Aebersold, 2003) as well as 2DE gels using immobilized pH gradient (IPG) strips in the first dimension and SDS-PAGE in the second dimension (Fig. 6). In addition, wild-type and *ffc* stroma were also analyzed by 2DE PAGE using native gels in the first dimension (CN-PAGE) and SDS-PAGE in the second dimension (Supplemental Fig. S3).

Comparative Analysis of the *ffc* and Wild-Type Chloroplast Stromal Proteomes from Mature Leaf Rosettes by ICAT

The stromal ICAT analysis was carried out with two biological replicates and included a label switch between the wild type and *ffc*. An overview of the procedure is provided in Figure 5, with an explanation provided in its legend. The two ICAT experiments identified 194 and 196 proteins, totaling 271 proteins (all identifications with associated scores and sequences are available via PPDB; Supplemental Table S1B). Since on average only about 20% of tryptic peptides contain a Cys, a significant proportion of the identified proteins were not quantified. A total of 293 and 133 ICAT-labeled peptide pairs were manually quantified in experiments 1 and 2, respectively (Supplemental Table S3, A and B). After removing peptides matched to proteins that did not pass the identification criteria, 267 and 126 peptides (experiments 1 and 2, respectively) were matched to 83 identified proteins (Supplemental Table S3C). We did not detect unlabeled Cys-containing peptides (even after searching for acrylamide adducts to Cys: propionamide C modification), indicating that the ICAT labeling was saturating. This was expected, as the ICAT reagent is an efficient alkylating reagent that was added in large excess. Forty-six proteins were quantified in both biological replicates (Table II), with an average CV for *ffc*/wild-type protein ratios of 14%. A few proteins were not quantified individually but as small clusters of closely related family members (Table II).

We focus on the 46 proteins that were quantified in both experiments and passed the strict identification filters (Table II). These proteins include members of the major biosynthetic pathways (Calvin cycle, pentose phosphate pathway, minor carbohydrates, starch, amino acids, chlorophyll, sulfur/Cys metabolism) as well as

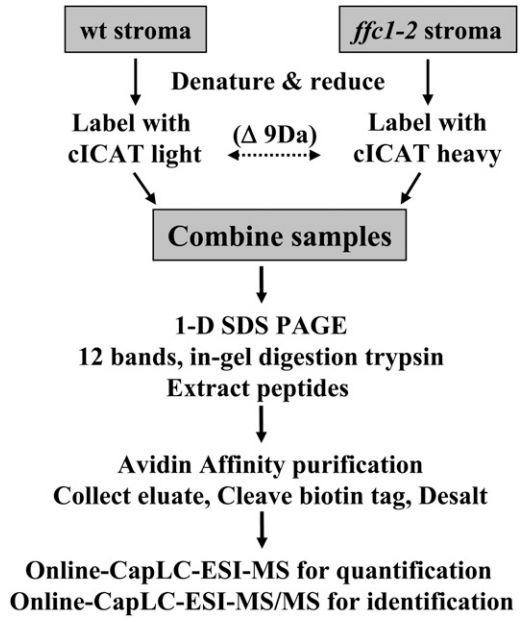

Figure 5. Schematic overview of the ICAT labeling experiments of wild-type and *ffc* chloroplast stroma. A total of 200 μg of each wild-type and *ffc* denatured stromal protein was labeled with the heavy or light ICAT tags. Mixed *ffc* and wild-type labeled proteomes were fractionated by one-dimensional SDS-PAGE and stained by Coomassie blue. The entire gel lane was cut into 12 gel slices, and proteins were digested with trypsin. After peptide extraction, ICAT-modified peptides were purified on an avidin column. After elution, the biotin tag was removed by acid cleavage and the peptide mixture was analyzed by reversed-phase nano-LC-ESI-MS. The 12 samples were first analyzed in MS mode to acquire an ion chromatogram for quantification and subsequently also in MS/MS mode for peptide identification. Peptides that lack Cys residues cannot be labeled with the ICAT method and eluted with the flow-through from the avidin columns. These unlabeled peptides were collected and analyzed by MS/MS to obtain better coverage of the stromal proteome.

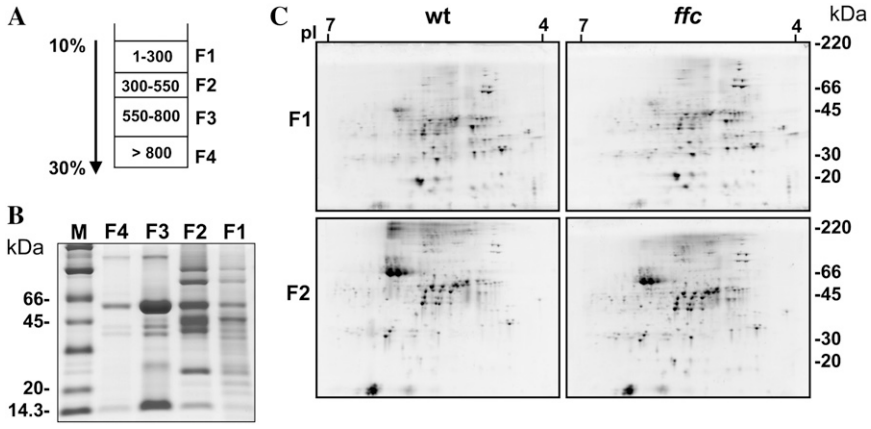

Figure 6. Suc gradient fractions and two-dimensional gels of wild-type and *ffc* plants. A, Schematic of Suc gradient fractionation, with molecular mass (MW) cutoff estimations in kilodaltons. F1, Monomers and low-molecular-mass complexes; F2, overlap fraction with Rubisco; F3, Rubisco-containing fraction; F4, high-molecular-mass fraction. B, One-dimensional SDS-PAGE of each fraction. C, Two-dimensional SDS-PAGE of F1 and F2 for wild-type and *ffc* plants.

protein synthesis and folding (CPN60, cpHSP70, and ROC4) and protein degradation (ClpC and zinc metalloprotease). While most of the *ffc*/wild-type protein ratios were close to 1, levels of 12 quantified Calvin cycle enzymes were systematically reduced in *ffc* (average *ffc*/wild type = 0.78 ± 0.10), which is consistent with the reduced LHC cross section and decrease in growth rates (see section below on the thylakoid). Stromal ascorbate peroxidase (At4g08390) was significantly increased by 56%, suggesting an increased level of hydrogen peroxide and consistent with 2-fold up-regulation of copper/zinc superoxide dismutase (CuZnSOD; At2g23190), as shown by 2DE gel analysis (see next section). It was also clear that there was no increased demand for either protein folding or stromal protein degradation, since the major chaperone systems Cpn60 and HSP70, as well as ClpC1 and -2 and the abundant stromal metalloprotease AtZnMP, accumulated at wild-type levels (Table II). We finally note that three ClpPR subunits of the major stromal Clp protease complex (quantified only in one of the biological replicates) were also at wild-type levels (Supplemental Table S3C).

Comparative Analysis of Chloroplast Stroma from Mature Leaf Rosettes by 2D-Isoelectric Focusing-SDS-PAGE

The CN-PAGE analysis of *ffc* and wild-type stroma did not show any obvious differences (Supplemental Fig. S3). The Rubisco holocomplex of approximately 550 kD represents 58% of the stromal protein mass in isolated chloroplasts from fully developed Arabidopsis leaf rosettes (Peltier et al., 2006). This strongly reduces the resolving power of 2DE gels using isoelectric focusing as the first dimension. Since our previous and current CN-PAGE gel analysis showed that most abundant stromal proteins are found in monomers or complexes below 550 kD (Peltier et al., 2006), we fractionated stroma from wild-type and *ffc* plants by Suc density centrifugation and collected proteins sedimenting above the Rubisco complex as two fractions (fractions 1 and 2). These two fractions were each focused in the first dimension on IPG strips and then separated by SDS-PAGE in the second dimension (Fig. 6). The experiment was carried out in duplicate using independent chloroplast preparations and including a technical replicate for fraction 1, resulting in 12 2DE gels. Protein spots were then matched across the 12 gels and quantified using image analysis software. The most abundant 150 spots were analyzed by peptide mass fingerprinting using matrix-assisted laser-desorption ionization time-of flight (MALDI-TOF) MS to ensure correct spot matching (data not shown) and to identify proteins in up- and down-regulated spots.

We were able to match and quantify 197 spots across fraction 1 and 109 spots across fraction 2, while 101 spots were matched and quantified across both fractions. Most spots did not show significant changes, consistent with the ICAT analysis of the stroma (presented above), showing that proteome homeostasis returned to steady state in fully developed leaves. However, we did find significant (>2-fold SD) changes for CuZnSOD (At2g28190) and an oxidoreductase-like protein of unknown function (At1g23740; Fig. 7). Both proteins likely relate to reactive oxygen species (ROS) defense and/or redox regulation (see "Discussion").

Comparative Analysis of the *ffc* and Wild-Type Thylakoid Proteomes from Mature Leaf Rosettes Using iTRAQ

The two independent stripped thylakoid preparations of wild type and *ffc* were digested with trypsin and labeled with iTRAQ reagents (114, 115, 116, and 117), and a label switch was included for each independent preparation (Supplemental Fig. S2). The two sets were fractionated by off-line SCX chromatography, and fractions were analyzed by nano-LC-ESI-MS/MS similar to the seedling samples, discussed above. This unambiguously identified 65 proteins with one or more uniquely matched peptides, and an additional nine proteins were identified as part of small protein families (Supplemental Table S1C; see PPDB). We quantified 42 proteins in both biological replicates, and only those are considered (Table III).

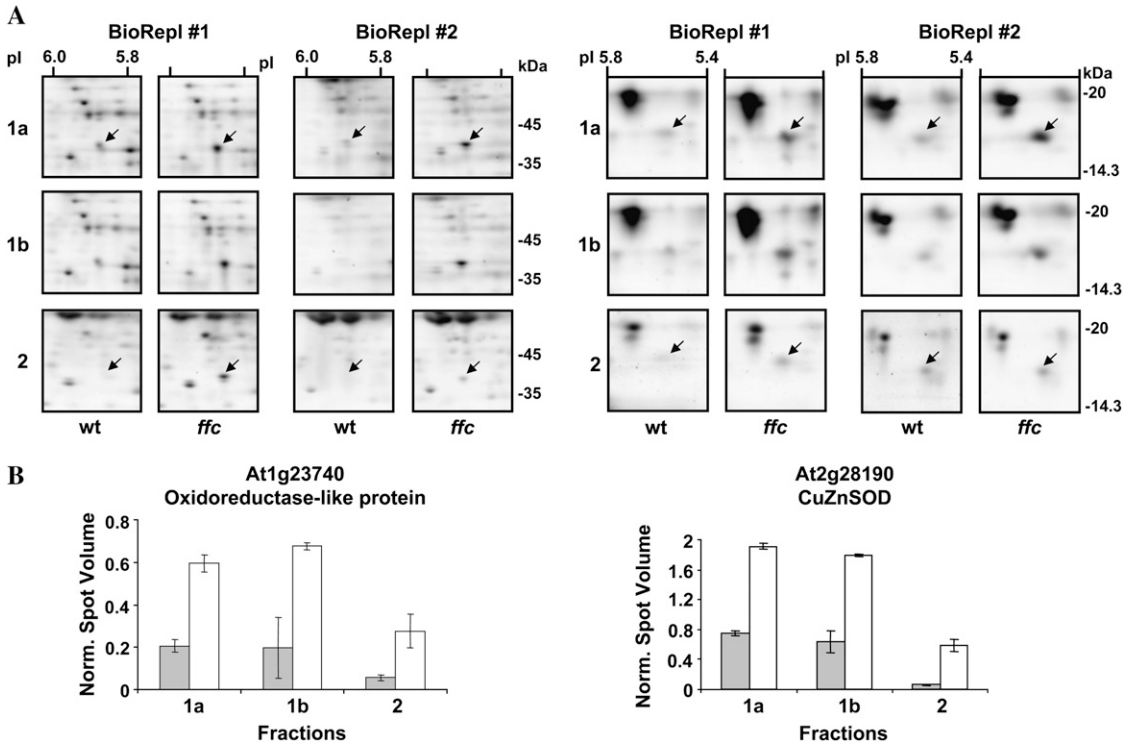

Figure 7. Identification of up-regulated proteins by two-dimensional gel analysis. A, Partial gel image of the corresponding up-regulated spot area for both At1g23740 and At2g28190. Fractions are indicated to the left of the gels. Fractions 1a and 1b correspond to technical replicates of fraction 1 (F1). Experimental molecular mass (in kilodaltons) is indicated to the right of the gels. B, Bar graph of normalized spot volumes for each protein. Gray bars, Wild type; white bars, *ffc*. SE bars represent a quantification average over 12 gels.

Accumulation levels of LHCI and major LHCII were reduced between 20% and 30% in *ffc*, while accumulation of the minor LHC proteins CP24, CP26, and CP29.1 was unaffected or even slightly increased. However, CP29.2 decreased by 40%. Accumulation levels of 10 quantified PSII core proteins in *ffc* increased on average by 12%, while the six quantified PSI core proteins decreased on average by 20%. Consequently, the PSI/PSII core ratio (determined by the average *ffc*/wild-type ratio for the core subunits) decreased by 30% in *ffc* as compared with the wild type in fully grown plants. Accumulation levels of subunits of ATP synthase and the cytochrome b_6f complex did not change. Interestingly, accumulation levels of thylakoid proteases FtsH2 and -8 doubled in *ffc*, suggesting an increased need for degradation of thylakoid proteins, similar to the findings in young seedlings (Table III).

Genetic Interaction between cpSRP54 and ClpC1

A central component in chloroplast protein biogenesis is the AAA^+ chaperone ClpC1 (At5g50920). ClpC1 predominantly accumulates in the chloroplast stroma, but it has also been shown to interact with the inner envelope protein import complex (Nielsen et al., 1997). A null mutant in *CLPC1* was isolated and has a virescent phenotype and reduced protein import rates (Constan et al., 2004; Kovacheva et al., 2005). A null mutant in a closely related homolog expressed at lower levels, ClpC2 (At3g48870), does not have any visible phenotype (Kovacheva et al., 2005). ClpC is not only involved in the chloroplast import process but also likely targets proteins to the ClpPR core complex for degradation (Adam et al., 2006; Sakamoto, 2006). It is conceivable that the functional association of ClpC with the Tic complex is to keep this major protein import pathway free from substrates that are trapped in the translocon. The comparative proteomics analysis of young *ffc* and wild-type seedlings described above, as well as previous western-blot data (Pilgrim et al., 1998; Hutin et al., 2002), showed that ClpC1 and -2 levels are increased by 30% to 50% in young *ffc* plants.

Given the relevance of ClpC1 in both import and degradation, we isolated a ClpC1 null mutant, *clpc1-1*, and crossed it with *ffc*. Double homozygous mutants were recovered in the F2 generation, and reverse transcription (RT)-PCR confirmed the lack of mRNA for both *cpSRP54* and *CLPC1* (Fig. 8). The double mutant was blocked in development after emergence of the cotyledons under autotrophic conditions, but it could be partially rescued under heterotrophic conditions (1% Suc; Fig. 8). Under these heterotrophic conditions, the double mutant developed and greened slowly and could eventually be transferred to soil. After about 9 months, the plants finally flowered and

Table III. *Quantified proteins in ffc and wild-type thylakoids of mature rosettes using iTRAQ with two biological replicates*

Protein Name[a]	Accession[b]	*ffc*/Wild-Type Ratio[c]	Curated Location[d]	Function
Lhcb1 and -2 subfamilies	AT1G29910.1 AT1G29920.1 AT1G29930.1 AT2G34420.1 AT2G34430.1 AT2G05100.1 AT2G05070.1 AT3G27690.1	**0.71 ± 0.17**	Thylakoid, integral	PSII antennae
LHCII-2.4	AT3G47470.1	**0.80 ± 0.01**	Thylakoid, integral	PSII antennae
LHCII-3	AT5G54270.1	0.79 ± 0.18	Thylakoid, integral	PSII antennae
Lhcb4.1 (CP29-1)	AT5G01530.1	**1.23 ± 0.09**	Thylakoid, integral	PSII antennae
Lhcb4.2 (CP29-2)	AT3G08940.2	**0.60 ± 0.05**	Thylakoid, integral	PSII antennae
LHCII-5 (CP26)	AT4G10340.1	**1.15 ± 0.07**	Thylakoid, integral	PSII antennae
LHCII-6 (CP24)	AT1G15820.1	1.04 ± 0.10	Thylakoid, integral	PSII antennae
LHCI-3 (LHCI-680A)	AT1G61520.1	**0.80 ± 0.10**	Thylakoid, integral	PSI antennae
PsbS	AT1G44575.1	**1.58 ± 0.02**	Thylakoid, integral	PSII antennae
PsbA D1	ATCG00020.1	1.23 ± 0.36	Thylakoid, integral	PSII core
PsbD D2	ATCG00270.1	1.17 ± 0.35	Thylakoid, integral	PSII core
PsbB CP47	ATCG00680.1	1.17 ± 0.09	Thylakoid, integral	PSII core
PsbC CP43	ATCG00280.1	**1.29 ± 0.06**	Thylakoid, integral	PSII core
PsbE cytochrome b559α	ATCG00580.1	1.08 ± 0.14	Thylakoid, integral	PSII core
PsbH-phospho	ATCG00710.1	0.98 ± 0.50	Thylakoid, integral	PSII core
PsbR	AT1G79040.1	0.89 ± 0.13	Thylakoid, integral	PSII core
PsbO OEC33	AT5G66570.1	1.24 ± 0.17	Thylakoid, lumenal side	PSII core
PsbO OEC33 and OEC33-like	AT3G50820.1 AT5G66570.1	1.26 ± 0.32	Thylakoid, lumenal side	PSII core
PsbP OEC23 Tat lTP	AT1G06680.1	1.31 ± 0.79	Thylakoid, lumenal side	PSII OEC
PsaA - subunit Ia	ATCG00350.1	0.83 ± 0.09	Thylakoid, integral	PSI core
PsaB - subunit Ib	ATCG00340.1	0.87 ± 0.11	Thylakoid, integral	PSI core
PsaD-1, -2	AT1G03130.1 AT4G02770.1	**0.80 ± 0.00**	Thylakoid, stromal side	PSI core
PsaE-1, -2	AT4G28750.1 AT2G20260.1	**0.80 ± 0.02**	Thylakoid, stromal side	PSI core
PsaF	AT1G31330.1	**0.78 ± 0.06**	Thylakoid, integral	PSI core
PsaG	AT1G55670.1	**0.71 ± 0.04**	Thylakoid, integral	PSI core
PsaH1, -2	AT1G52230.1 AT3G16140.1	**0.66 ± 0.12**	Thylakoid, integral	PSI core
PsaL	AT4G12800.1	0.95 ± 0.32	Thylakoid, integral	PSI core
PSI-P - TMP14 (pTAC8)	AT2G46820.1	1.38 ± 0.31	Thylakoid	PSI core
PetA - cytochrome *f*	ATCG00540.1	1.34 ± 0.17	Thylakoid, integral	Cytochrome b_6/f
PetB - cytochrome b_6	ATCG00720.1	0.88 ± 0.28	Thylakoid, integral	Cytochrome b_6/f
PetC - Rieske iron-sulfur	AT4G03280.1	1.17 ± 0.11	Thylakoid, lumenal side	Cytochrome b_6/f
CF1a - atpA	ATCG00120.1	0.90 ± 0.43	Thylakoid, stromal side	ATP synthase
CF1b - atpB	ATCG00480.1	0.98 ± 0.87	Thylakoid, stromal side	ATP synthase
CF1e - atpE	ATCG00470.1	1.31 ± 0.66	Thylakoid, stromal side	ATP synthase
CF1y - atpC	AT4G04640.1	1.19 ± 0.16	Thylakoid, stromal side	ATP synthase
CFO-I - atpF	ATCG00130.1	**0.71 ± 0.04**	Thylakoid, integral	ATP synthase
CFO-II - atpG	AT4G32260.1	1.04 ± 0.22	Thylakoid, integral	ATP synthase
FNR-1	AT5G66190.1	1.71 ± 0.36	Thylakoid, stromal side	Ferredoxin reductase
Fibrillin (FIB4)	AT3G23400.1	1.50 ± 0.53	Plastoglobules; thylakoid, stromal side	Fibrillin
FtsH2/8	AT1G06430.1 AT2G30950.1	1.98 ± 0.55	Thylakoid, integral	Protein degradation
TL18.3	AT1G54780.1	**1.36 ± 0.16**	Thylakoid, lumenal side	Unknown function lumen
Expressed protein	AT5G23060.1	0.94 ± 0.51	Thylakoid, integral	Unknown thylakoid

[a]Down-regulated or up-regulated proteins are marked in boldface (at least 2 SD away from unity). [b]Some labeled peptides matched to one or more close homologues (e.g. the LHCII family); these homologues are listed. They are underlined if the accession was quantified with only shared peptides. [c]Average ratios with SD. Numbers marked in boldface are up-regulated or down-regulated and at least 2 SD away from unity.

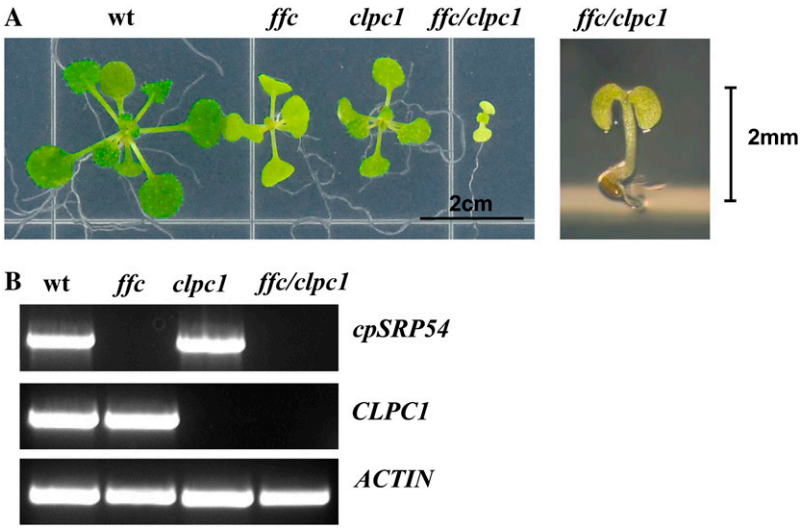

Figure 8. Phenotype and mRNA accumulation levels of wild type, *clpc1*, *ffc1*, and *clpc1 ffc* plants. A, Twenty-four-day-old plants grown on half-strength MS medium containing 1% Suc. Wild-type plants are at stage 1.08, *ffc* and *clpc1* plants are at stage 1.05, and *ffc clpc1* plants are at stage 1.02. The right panel shows the seedling-lethal phenotype of a *clpc1 ffc* double mutant plant grown for 30 d on half-strength MS medium without Suc. B, RT-PCR of cpSRP54 and CLPC1 for each genotype. *ACTIN* was used as an internal control.

produced low amounts of viable seed. The strong phenotype confirms the significance of the iTRAQ-based quantification in young seedlings and indicates that ClpC1 is of particular importance when intraplastid sorting is disturbed.

DISCUSSION

Protein sorting is a key process in the development and function of eukaryotic and prokaryotic organisms; disruption of this process often leads to developmental and functional defects. Since protein sorting is so vital, redundancies are often built in, while various rescue mechanisms are in place to either remove missorted and aggregated proteins through proteolysis or rescue them via chaperones (Bukau et al., 2006). Therefore, to study protein-sorting pathways and the consequences of inactivation of specific sorting components, an integrative approach is needed that can monitor many of the protein homeostasis components as well as other cellular functions in parallel. Gel-based and, in particular, MS-based techniques to determine quantitative differences between proteomes have greatly improved in recent years (Goshe and Smith, 2003; Domon and Aebersold, 2006; Bantscheff et al., 2007), and several of these comparative and quantitative techniques have been used to study plants (for review, see Jorrin et al., 2007; Thelen and Peck, 2007). We present a comparative proteomics approach to address the intrachloroplast sorting and homeostasis network and to determine the cellular response outside of the chloroplast.

Quantitative Proteomics Methodologies for Analysis of Chloroplast and Other Mutants Affecting Leaf Development

We used MS-based (iTRAQ and ICAT) and 2DE gel-based quantification techniques to study the impact of cpSRP54 deletion in both young seedlings and mature rosettes (see Fig. 3 for overview). To analyze young seedlings, we optimized a procedure for the extraction of total cellular proteins, including membrane and soluble proteins, avoiding any gel-based steps. Proteins were extracted with SDS and could be efficiently digested after solubilization in dimethyl sulfoxide (DMSO), as we previously demonstrated for the plastoglobule proteome (Ytterberg et al., 2006). Importantly, membrane proteins were well represented using this method. This gel-free digestion procedure is also particularly attractive when using the iTRAQ peptide-labeling technique. Since the *ffc* mutant is affected in leaf and chloroplast development (Figs. 1 and 2), we included a comparison based on similar leaf age as well as similar leaf growth stage. This was important, as even a difference of 4 d in plant age significantly affected thylakoid composition in these young seedlings (but not other compartments; Table I). The seedling analysis identified and quantified mostly chloroplast proteins (60%), making this an attractive general method for the analysis of chloroplast mutants, especially if these mutants have strong phenotypes from which it may be difficult to isolate significant amounts of intact chloroplasts.

For a more detailed analysis of the purified chloroplast stromal proteome isolated from fully developed leaf rosettes, we used ICAT (Table II; Fig. 5), as well as 2DE gel analysis (Figs. 6 and 7). To overcome the loss of resolution by the presence of high amounts of Rubisco, we used a simple and reproducible Suc gradient fractionation step prior to 2DE gel analysis. The ICAT and 2DE gel analysis was complementary and consistently showed that protein homeostasis reached steady state without folding or degradation "stress." The CVs of quantified protein ratios across biological replicates using the iTRAQ and ICAT methods were very similar (14%–15%). A clear disadvantage of the ICAT method was that a significant number of identified proteins could not be quantified due to dependence on the presence of Cys.

The Posttranslational SRP Sorting Machinery, But Not the SecY/E Translocon, Is Down-Regulated upon Development

Protein import and sorting rates are particularly high during early leaf and chloroplast development to sustain rapid cell division and expansion. As the leaf matures, import and sorting slow down and the leaf proteome reaches steady state. We found that protein accumulation levels of cpSRP54, cpSRP43, cpFtsY, and ALB3, but not SecY/E, decreased during leaf development when based on total protein concentration (Fig. 2) and even more if chlorophyll concentration was used for normalization. Down-regulation of these SRP targeting components with progressive leaf development has not been shown before but is consistent with a decreasing need for this biogenesis machinery as more of the thylakoid membrane system is developed. When seedlings of the same developmental stage were compared, levels of each of these sorting components were similar. The relatively stable accumulation levels of the SecY/E translocon are in contrast to the down-regulation of the SRP pathway components. This suggests that the Sec translocon has a sustained role in chloroplast proteome homeostasis, possibly to accommodate the D1 synthesis and repair cycle of PSII (Aro et al., 2005).

Substrates for cpSRP54 in the LHC Family and Significance of the L18 Domain

We quantified a number of LHC proteins in both young seedlings and developed rosettes. All LCH proteins were reduced except for CP26 in young seedlings, while in fully developed rosettes all quantified LHCs except for CP24, CP26, and CP29-1 were reduced. In particular, these minor LHCII proteins accumulated at higher levels in fully developed rosettes, which is consistent with western-blot analysis (Amin et al., 1999). This also supports the idea that sorting can proceed using only cpSRP43 when cpSRP54 (normally interacting with LHC substrate via hydrophobic TMDs) is not present, in agreement with previous observations (Amin et al., 1999; Hutin et al., 2002; Tzvetkova-Chevolleau et al., 2007).

While it has been established that the L18 domain is required for cpSRP43 interaction (for review, see Schunemann, 2004), it is not clear which residues within the L18 domain are important. From the alignment of the L18 domains of all Arabidopsis LHC proteins, we observed that the L18 domain is generally conserved but that a number of LHCs, in particular the CP29 family, CP26, and LHCI-1.1, have one or more basic residues upstream or downstream of the central YPGG domain; this changes the overall properties of this cpSRP43 interaction domain (Fig. 4). One could argue that in the absence of the LHC interaction with cpSRP54, the properties of the L18 domain determine how successful LHC can still be targeted to the thylakoid membrane via cpSRP43 alone, thus providing an explanation for the behavior of most minor LHCIIs. However, CP29.2 and LHCI-1 did not follow this pattern, indicating that features other than the L18 domain in the LHCs contribute to the efficiency to bypass cpSRP54.

Consequences for Chloroplast-Encoded Proteins and Decreased PSI/PSII Core Ratio

The most pronounced and persistent effect on the thylakoid proteome was the reduction in accumulation of PSI core subunits and, consequently, a decrease in PSI/PSII ratio. The strong effects on these PSI subunits are consistent with immunoblot data for PsaA and -B in previous in vivo studies (Pilgrim et al., 1998; Amin et al., 1999). These two chloroplast-encoded reaction center proteins are very hydrophobic (GRAVY index 0.25 and 0.12, respectively), with nine to 11 TMDs, and their biosynthesis and membrane assembly are likely sensitive to aggregation. The reduced accumulation of these two chloroplast-encoded proteins is most likely a consequence of their cotranslational dependence on cpSRP54, although direct evidence is lacking. In contrast, the decline in accumulation of the nucleus-encoded PSI subunits may not be directly related to the loss of sorting efficiency; rather, it could be a consequence of the reduced accumulation of PsaA and -B and subsequent degradation by the thylakoid membrane proteases. Indeed, we found that thylakoid FtsH1 and -5 proteins were up-regulated in both young and fully developed leaf rosettes (Tables I and III). The lower steady-state PSI/PSII ratio could also be a consequence of the reduced cross section of the PSII antennae. In addition, there appear to be changes in the relative contributions of the minor LHC members (CP42, CP26, and CP29), which may affect the efficiency of the LHCII antennae, thus affecting the PSI/PSII balance.

The *ffc* Phenotype Changes during Progressive Leaf and Chloroplast Development

The proteomics analysis of the *ffc* mutant showed that the protein homeostasis machinery and the Calvin cycle enzymes responded differently in young as compared with mature leaves (Tables I and II). In particular, cpSRP54 deletion led in young leaves to up-regulation of thylakoid proteases and stromal chaperones, including ClpC, and various RNA-binding proteins. The RNA-binding proteins have been shown to be vital for the stability of chloroplast mRNA, and they have been suggested to be global mediators of chloroplast RNA metabolism, connecting transcription and translation in chloroplasts (Nakamura et al., 2004). In contrast, the stromal protein homeostasis machinery returned to wild-type levels in mature leaves, consistent with the developmental down-regulation of the SRP pathway. A differential response between young and mature leaves was also found in carbon metabolism, with an up-regulation of the Calvin cycle,

the envelope triosephosphate translocator (Weber et al., 2005), and the photorespiratory pathway in peroxisomes and mitochondria. Since photorespiration exports reducing equivalents from the chloroplasts, this suggests a low ATP/NADPH production ratio by the photosynthetic light reaction. The up-regulation of most Calvin cycle enzymes is best explained by a partial uncoupling or insufficient coordination between expression of the Calvin cycle enzymes and thylakoid biogenesis during periods of rapid cell growth and division. In contrast, the Calvin cycle was down-regulated in mature leaves, likely to adjust to the reduced capacity of the light reaction, while ROS defense proteins (CuZnSOD, stromal ascorbate peroxidase, and the uncharacterized oxidoreductase-like protein) were up-regulated. This increase in ROS defense points to the production of superoxide/hydrogen peroxide, consistent with a low ATP/NADPH production ratio. This may well relate to the decreased PSI/PSII ratio and, consequently, a reduced cyclic electron flow capacity. These secondary effects of cpSRP54 deletion were otherwise confined to the chloroplast, since cytosolic glycolysis, nitrogen transport, and SAM cycle proteins, involved in the biosynthesis of Met and SAM, did not change.

The double mutant *ffc clpc1* showed a much stronger phenotype than either single mutant (Fig. 8), which confirms the significance of ClpC up-regulation in young leaves. It has been shown that ClpC interacts in a reversible manner with the Tic translocon (in particular Toc110; Nielsen et al., 1997; Kovacheva et al., 2007) and that loss of ClpC1 decreases the import efficiency of various substrates (Constan et al., 2004; Kovacheva et al., 2005). ClpC likely assists the translocation of substrates by pulling the substrate out of the translocon in an ATP-dependent manner. LHC sorting to the thylakoid is clearly less efficient, and ClpC could help to keep this major protein import pathway free from substrates that are trapped in the translocon. The observed increases in CPN60 and HSP70 support a role in LHC stabilization, possibly compensating for the lack of stabilization by cpSRP54.

MATERIALS AND METHODS

Generation and Genotyping of Single and Double Mutants, Plant Growth, and Treatments

The *ffc* mutant previously characterized (Amin et al., 1999) was originally isolated from an ethyl methanesulfonate mutagenesis screen and shown to have an approximately 10-kb insertion in intron 8 of the gene encoding cpSRP54 (At5g03940.1). The *clpc1* mutant is a T-DNA insertional mutant in At5g50920 in the Columbia (Col-0) ecotype obtained from the SALK collection (SALK_014058). The T-DNA is inserted in the fourth exon, at 1,332 bp from the start codon, which was confirmed by DNA sequencing. The *ffc* mutant was crossed to *clpc1*, and the F2 population was screened on soil in short days (10 h of light, 14 h of dark). No double homozygotes were found, but screening the F2 population on half-strength Murashige and Skoog (MS) plates containing 1% Suc in short days identified an *ffc clpc1* double mutant. *ffc clpc1* double mutant plants exhibit seedling lethality when grown only on MS medium without Suc in short days. mRNA levels in wild-type, *clpc1*, *ffc*, and *ffc clpc1* plants were determined from 24-d-old plants grown in short days on half-strength MS medium containing 1% Suc by RT-PCR. Total RNA was isolated from approximately 100 mg of tissue from these plants using Tri-Reagent (Molecular Research Center). cDNA was amplified from 2 μg of total leaf RNA with SuperScript III (Invitrogen). Primers for cpSRP54 (forward, 5′-GAGGCTCTTCAATTTTCCAGCG-3′; reverse, 5′-CAGGCTTGCTTGATGCTGACTC-3′) were used to amplify the entire coding sequence of 1,663 bp. Primers for CLPCl (forward, 5′-ATGGCTATGGCCACAAGGGTGTTG-3′; reverse, 5′-GATCTTCTGGGTACAGCTCACAATATTG-3′) were used to amplify a 1,024-bp segment at the N-terminal portion of the gene.

For chloroplast isolation, stroma purification, thylakoid preparation, and total plant protein isolation, wild-type (Col-0) and *ffc* plants were grown on soil under a 10-h-light/14-h-dark period at 22°C/19°C at 280 μmol photons m^{-2} s^{-2}.

Preparation of Whole Leaf Extracts from Different Leaf Stages for Immunoblot Analysis

Individual leaf pairs at defined stages were collected and frozen in liquid nitrogen. Around 20 to 30 leaves were pooled for small leaves (2–5 mm), around eight to 10 for medium-sized leaves (5–10 mm), and two to six for big leaves (<10 mm). Frozen leaves were ground with mortar and pestle in 500 μL of medium containing 50 mM Tris-HCl (pH 6.8), 2 mM EDTA, and 50 μg mL^{-1} water-soluble irreversible Ser protease inhibitor Pefablok [(4-(2-aminoethyl) benzenesulfonyl fluoride hydrochloride; Biomol] and subsequently filtered through nylon mesh (22 μm). Proteins were then either precipitated in 80% acetone (the supernatant was used to determine chlorophyll concentrations [Porra et al., 1989]) or thylakoid membranes were collected by centrifugation at 12,000*g* for 3 min. Protein pellets were solubilized in 50 to 100 μL of 5% SDS and 50 mM Tris-HCl (pH 8.3), and thylakoid membrane pellets were solubilized in 100 μL of 6 M urea, 5% SDS, 0.3 M Suc, and 50 mM Tris-HCl (pH 8.3).

Before starting the western-blotting analysis of the leaf pairs, titrations were carried out to determine the linearity of the antibodies directed against cpSRP54, cpSRP43, cpFtsY, cpSecY, and ALB3 using wild-type and *ffc1-2* leaf material from young leaves (data not shown). Based on these titrations, 50 μg of total leaf protein extract was loaded for analysis of cpSRP54, 20 μg for cpSRP43, and 30 μg for cpFtsY and ALB3. Thylakoid membranes corresponding to 100 μg of total leaf protein extract were loaded for analysis of cpSecY and cpSecE. A fragment of ALB3 (amino acids 327–462) was overexpressed in *Escherichia coli*, gel purified, and injected into rabbits for the production of polyclonal antiserum (AgriSera), and the serum was used at 1:1,000. Generation of cpSecE serum has been described (Froderberg et al., 2001). Rabbit polyclonal antisera raised against cpSecY (used at 1:2,000), cpFtsY (used at 1:2,000), and cpSRP54 (used at 1:1,000) were kind gifts from Neil E. Hoffmann. The cpSRP43 sera (used at 1:3,000) were kind gifts of Laurent Nussaume and Ralph Henry. Proteins were separated on 12% or 14% Laemmli SDS-PAGE gels containing 6 M urea and blotted onto polyvinylidene difluoride membranes. For cpSecE, proteins were separated on an 8% to 16% gradient Tricine SDS-PAGE gel containing 6 M urea and blotted onto a polyvinylidene difluoride membrane. Bound primary antisera were detected with secondary antibodies conjugated to horseradish peroxidase (Sigma) and detected by enhanced chemiluminescence.

Isolation of Total Cellular Proteome for Seedling Analysis by iTRAQ

Proteins from total tissue were isolated from wild-type and *ffc* seedlings at growth stage 1.07 (wild type and *ffc* at 17 and 21 d, respectively) and for wild-type seedlings at growth stage 1.11 (wild type at 21 d). Ten seedlings (leaf tissue only) of each developmental stage and genotype were ground in extraction buffer (6 M urea, 5% SDS, 0.3 M Suc, 50 mM Tris-HCl, pH 8.3, and 5 mM tributylphosphine) in a mortar. The supernatant was filtered through a 45-μm Miracloth, and insoluble material was removed by centrifugation at 18,000*g* for 1 min at 4°C. Each sample was precipitated in 80% or 100% acetone at −20°C. The protein pellets were collected by centrifugation at 18,000*g* for 5 min at 4°C followed by solubilization in 2% SDS and protein determination using the bicinchoninic acid method (Smith et al., 1985).

Isolation of the Stripped Thylakoid Proteome for Analysis by iTRAQ

Thylakoids were purified from fully developed leaves using a combination of differential and gradient centrifugation steps as described previously (Friso et al., 2004). Soluble and peripheral proteins were removed by stripping the

thylakoid membrane as follows: thylakoid membranes were resuspended at 10 mg chlorophyll mL^{-1} in ice-cold 10 mM HEPES-KOH (pH 8.0) buffer containing a cocktail of protease inhibitors as listed (Peltier et al., 2002). The suspension was diluted 20 times with ice-cold solutions of 2 M KBr and KNO_3 to a final concentration of 1 M. The suspension was stirred slowly for 30 min on ice with 10-s sonication steps every 5 min. Membranes were collected by centrifugation at 150,000*g* for 25 min at 4°C, washed with 10 mM HEPES-KOH (pH 8.0) buffer with sonication to remove the remaining salts, followed by centrifugation at 150,000*g* for 15 min to collect the stripped membranes. The membranes were then solubilized with 50 mM Tris-HCl (pH 8.0), 3 M urea, and 2% SDS.

Removal of SDS, Digestion in Solution, and iTRAQ Labeling

A total of 30 μg of protein from each sample was incubated overnight at −20°C with 450 μL of 100% acetone followed by centrifugation (18,000*g*, 4°C, 15 min), washing the pellet with 80% acetone, 10% methanol, 0.2% acetic acid, and 9.8% water in acetone, followed by 30 min of incubation at −20°C, followed by a final centrifugation (18,000*g*, 4°C, 15 min) to collect the protein. The proteins were solubilized in 20 μL of 100% DMSO, followed by dilution with digestion buffer to a final concentration of 50 mM ammonium bicarbonate and 30% DMSO. After adding trypsin to a protein:trypsin ratio of 20:1 (and a final volume of 67 μL), the samples were incubated on a shaker overnight at 37°C. After digestion, the DMSO was removed by evaporation in a SpeedVac and the peptides were dissolved in 100 μL of 5% formic acid (FA). A total of 13 μg (43.3 μL) from each sample was divided into aliquots in two tubes and dried down. A total of 100 μL of water was added to each tube and evaporated to remove residual ammonium bicarbonate. Then, 30 μL of 0.5 M triethyl ammonium bicarbonate was added to each tube and vortexed. Each peptide sample was mixed with a whole tube of labeling iTRAQ reagent (114, 115, 116, or 117; Applied Biosystems) and incubated on a shaker at room temperature for 1 h. The samples to be compared were pooled, and 50 μL of 5% FA per sample was added per label to set the pH. Finally, the solutions were diluted to 10 times the reaction volume with 25% acetonitrile (ACN) and 1% FA (final concentration $<$ 0.05 M triethylammonia bicarbonate).

SCX Chromatography of iTRAQ-Labeled Samples

The iTRAQ-labeled peptides were separated using SCX chromatography on a PolySULFOETHYL A column (200 × 2.1 mm, 5 μm, 300 Å) from PolyLC connected to an Agilent 1100 HPLC system. Solution A was 25% ACN and solution B was 25% ACN and 0.5 M ammonium formate (pH 3.0, set with FA). A total of 100 μL of each sample was injected five times (3% B, 0–3 min) before eluting the peptides off the column at a flow rate of 200 μL min^{-1} as follows: 3% B, 0 to 10 min; 3% to 10%, 10 to 15 min; 10% to 60%, 15 to 20 min; 60% to 100%, 20 to 25 min; 100%, 25 to 35 min; 100% to 3%, 35 to 37 min; 3%, 37 to 45 min. The fractions were collected on microtiter plates (start at 2 min, end at 45 min; 1 min per fraction; approximately 3-min dead volume). The fractions were lyophilized and resuspended with 5% FA.

MS Analysis of iTRAQ Samples

For identification and quantification, the eight SCX fractions containing the majority of the peptides (fractions 23–30) were analyzed by data-dependent on-line tandem MS using CapLC-ESI-MS/MS (Q-TOF1; Waters), as described previously (Zybailov et al., 2008). Proteins were identified by searching the MS data against the ATH1v6 database concatenated with a decoy in which all sequences were in reverse orientation using Mascot with a significance threshold of 0.01. The maximum mass error tolerance for precursor and product ions was set at 1.2 and 0.8 D, respectively. Search criteria were as follows: full tryptic peptides only, variable Met oxidation, fixed iTRAQ modification for N termini and Lys residues, and variable iTRAQ modification for Tyr residues. In addition, only MS/MS spectra with ion scores of 20 or higher were considered for identification, although lower ion scores were allowed for quantification.

Calculation of Protein Ratios and Quality Control of iTRAQ Data

Mascot distiller was used to calculate peak areas and extract mass-to-charge ratio values of the precursor ions, areas, and retention times. The peak areas of the reporter ions were extracted and then corrected for label purity with parameters supplied by Applied Biosystems using a program written by Dr. Qi Sun (Theory Center, Cornell University). The quantified reporter ion information for each fragmented precursor ion was coupled to the queries matched to protein accessions; quantifications for queries that were not used for identification were removed. When queries were used to identify more than one peptide, only the best match (i.e. the best interpretation of the spectrum) was kept, unless it seemed that more than one peptide was fragmented at the same time. In the latter case, the spectrum was used for the normalization but discarded for the statistical analysis of the proteins, since the reporter ions would originate from two different sources. After normalization, the peptides were grouped according to peptide sequence and the areas of reporter ions originating from the same peptide sequence were added together (i.e. repeated fragmentation of the same ion, or fragmentation of peptides with different modifications such as oxidized Met) to prevent one peptide sequence from biasing the protein average. The peptides were then grouped according to the proteins they matched. The sequences of the proteins that had shared peptides were aligned using Multi-align (Corpet, 1988), and the peptide sequence was matched to the alignment to clarify the peptide-protein relationship. Unique and shared peptides were kept separate to not compromise the data, and averages and SD values for the individual biological replicates were calculated using the ratios from the labeling experiments. Outliers were removed conservatively using the SD.

2D-PAGE Analysis of Chloroplast Stroma of *ffc* and Wild-Type Plants

Isolation of chloroplasts and extraction of stromal proteins were carried out as described (van Wijk et al., 2007). A total of 2 mg of purified total concentrated stroma from both wild-type (Col-0) and *ffc* chloroplasts was loaded onto a 2-mL 10% to 30% continuous Suc gradient (in 10 mM HEPES-KOH, pH 8.0, 5 mM $MgCl_2$, and protease inhibitors). Gradients were spun at 4°C for 3 h at 55,000 rpm in an ultracentrifuge (Beckman-Coulter) and manually fractionated at 4°C into four fractions. A total of 150 μg of protein from fraction 1 and fraction 2 was precipitated in 80% acetone, resuspended in rehydration buffer (final concentration), and rehydrated onto 11-cm pI 4 to 7 IPG strips (Amersham Pharmacia). Strips were focused in the first dimension, reduced, alkylated, and run in the second dimension on 8% to 16% Tris-HCl Criterion gels (Bio-Rad). Gels were fixed in 10% methanol and 7% acetic acid for 1 h and stained with Sypro Ruby O/N. Gels were then destained in fix solution and rinsed with double-distilled water for 15 min, and images were acquired with a Fluor-S unit (Bio-Rad). Spot quantification was performed using Phoretix 2D software. Final spot volumes were normalized to total gel volume for each gel. Stained gel spots were excised manually or using a ProPic robot (Genomic Solutions). The spots were washed, digested with modified trypsin (Promega), and extracted using a ProGest robot (Genomic Solutions). The extracted peptides were dried and resuspended in 15 μL of 5% FA. Protein identification was performed by peptide mass fingerprinting using MALDI-TOF MS in reflectron mode (Voyager DE-STR; Perseptive Biosystems). Peak lists (mgf files) from the MALDI data were generated using MoverZ software *m/z* (Freeware edition; Proteometrics) using a minimum signal-to-noise ratio of 3.0 and peak resolution of 5,000. The peak lists were searched against Athv6 using Mascot version 2.2 with a maximum *P* value of 0.05. Criteria for positive identification by MALDI-TOF MS peptide mass fingerprinting included five or more matching peptides with a narrow error distribution (clustering of errors) within 25 ppm and at least 15% sequence coverage. Only peptides without missed cleavages (by trypsin) were considered, with Met oxidation as variable modification and carbamido methylation as fixed modification. In exceptional cases (i.e. proteins of less than 20 kD and matching gel coordinates), four matching peptides were considered as positive identification.

Stable Isotope Labeling Using ICAT and MS Analysis

A total of 200 μg of purified stromal proteins from wild-type and *ffc* plants was denatured and reduced using 50 mM TCEP-HCl. All Cys residues were labeled with the light (containing only ^{12}C stable isotopes) or heavy (^{13}C) ICAT reagent according to the manufacturer's instructions (Applied Biosystems). Labeling reactions were performed separately by incubation at 37°C for 2 h. After labeling, the samples were combined and proteins separated by one-dimensional SDS-PAGE (12% acrylamide), followed by Coomassie Brilliant Blue R-250 staining. The gel lane containing the ICAT-labeled samples was

completely cut into 12 slices. Each slice was cut into 1-mm^3 pieces, washed, and digested with modified trypsin (Promega), and the resulting peptides were eluted principally as described (Shevchenko et al., 1996). After vacuum concentration, 30 μL of 25% ACN, 5 mM KH_2PO_4, 350 mM KCl (pH 2.7), and 500 μL of affinity-loaded buffer (pH 7.2) were added to each sample as described (Li et al., 2003). The biotin-tagged peptides were purified on avidin columns as instructed by the manufacturer. Protein digests were qualitatively analyzed by MALDI-TOF MS (Voyager DE-STR; Applied Biosystems) to confirm total digestion and/or labeling. Labeled peptides were then loaded on a guard column (LC Packings; MGU-30-C18PM), followed by separation on a PepMap C18 reversed-phase nano column (LC Packings nan75-15-03-C18PM), using 90-min gradients with 95% water, 5% ACN, and 0.1% FA (solvent A) and 95% ACN, 5% water, and 0.1% FA (solvent B) at a flow rate of 200 nL min^{-1}. The labeled peptide mixtures were analyzed by LC-ESI-MS/MS (Q-TOF1). Each ICAT-labeled sample was run in duplicate under the same chromatographic settings. For protein quantification, the samples were first analyzed in MS mode and the areas of the peptides were calculated using Masslynx 4.0 SP1. The second run was set up for data-dependent MS/MS acquisition for protein identification. The flow-through from the 12 avidin column purifications (containing nonlabeled peptides, i.e. peptides without Cys residues) was also collected and analyzed by MS/MS (peptides not usable for quantification but valuable for protein identification) after off-line desalting on C18 microcolums (Gobom et al., 1999). The experiment was carried out in duplicate with independent chloroplast preparations and "label switch" to avoid a possible bias due to the ICAT label. All quantified peptides and details are listed in Supplemental Table S3. Criteria for protein identification were similar to those for the iTRAQ-labeled peptides, except that a variable ICAT modification was included (instead of variable iTRAQ modification).

The PPDB

MS-based information for all identified proteins listed in Supplemental Table S1 was extracted from the Mascot search pages and filtered for significance (e.g. minimum ion scores, etc.), ambiguities, and shared peptides as described (Zybailov et al., 2008). This information includes Mowse score, number of matching peptides, number of matched MS/MS spectra (queries), number of unique queries, highest peptide score, highest peptide error (in ppm), lowest absolute error (ppm), sequence coverage, and tryptic peptide sequences. This information is available using the search function "Proteome Experiments" and selecting the desired output parameters; this search can be restricted to specific experiments. Alternatively, information for specific accessions (either individually or a group) can be extracted using the search function "Accessions," and if desired, this search can be limited to specific experiments. Finally, information for a particular accession can also be found on each "Protein Report Page." The Map-Man Bin system (Thimm et al., 2004) is used for functional assignment, and all assignments for identified proteins were verified manually.

Supplemental Data

The following materials are available in the online version of this article.

Supplemental Figure S1. Protein-to-chlorophyll *a*/*b* ratios (w/w) of cotyledons and leaf pairs 1/2, 3/4, 5/6, 7/8, and 11/12 at developmental stages 1.08 and 1.12 of wild-type and *ffc* plants.

Supplemental Figure S2. Experimental design of iTRAQ experiments.

Supplemental Figure S3. CN-PAGE of chloroplast stroma from fully developed leaf rosettes of wild-type and *ffc* plants.

Supplemental Table S1. Identification and annotation of identified proteins in seedlings (A), stroma (B), and thylakoids (C) obtained from chloroplasts isolated from fully developed leaf rosettes.

Supplemental Table S2. Quantification data of total seedling leaf proteomes of *ffc* and wild-type plants by iTRAQ.

Supplemental Table S3. ICAT-based quantification of chloroplast thylakoid proteins from fully developed *ffc* and wild-type leaf rosettes.

Supplemental Table S4. iTRAQ-based quantification of chloroplast thylakoid proteins from fully developed *ffc* and wild-type leaf rosettes.

Supplemental Program S1. Program for the correction of iTRAQ purity.

ACKNOWLEDGMENTS

We thank Jitae Kim for the design and testing of *CLPC* primers and other members of the van Wijk laboratory for help and discussions. We thank Neil E. Hoffmann, Laurent Nussaume, and Ralph Henry for generous gifts of antisera.

Received June 11, 2008; accepted July 4, 2008; published July 16, 2008.

LITERATURE CITED

Adam Z, Rudella A, van Wijk KJ (2006) Recent advances in the study of Clp, FtsH and other proteases located in chloroplasts. Curr Opin Plant Biol **9:** 234–240

Amin P, Sy DA, Pilgrim ML, Parry DH, Nussaume L, Hoffman NE (1999) Arabidopsis mutants lacking the 43- and 54-kilodalton subunits of the chloroplast signal recognition particle have distinct phenotypes. Plant Physiol **121:** 61–70

Aro EM, Suorsa M, Rokka A, Allahverdiyeva Y, Paakkarinen V, Saleem A, Battchikova N, Rintamaki E (2005) Dynamics of photosystem II: a proteomic approach to thylakoid protein complexes. J Exp Bot **56:** 347–356

Bantscheff M, Schirle M, Sweetman G, Rick J, Kuster B (2007) Quantitative mass spectrometry in proteomics: a critical review. Anal Bioanal Chem **389:** 1017–1031

Boyes DC, Zayed AM, Ascenzi R, McCaskill AJ, Hoffman NE, Davis KR, Gorlach J (2001) Growth stage-based phenotypic analysis of *Arabidopsis*: a model for high throughput functional genomics in plants. Plant Cell **13:** 1499–1510

Bukau B, Weissman J, Horwich A (2006) Molecular chaperones and protein quality control. Cell **125:** 443–451

Chandrasekar S, Chartron J, Jaru-Ampornpan P, Shan SO (2008) Structure of the chloroplast signal recognition particle (SRP) receptor: domain arrangement modulates SRP-receptor interaction. J Mol Biol **375:** 425–436

Constan D, Froehlich JE, Rangarajan S, Keegstra K (2004) A stromal Hsp100 protein is required for normal chloroplast development and function in Arabidopsis. Plant Physiol **136:** 3605–3615

Corpet F (1988) Multiple sequence alignment with hierarchical clustering. Nucleic Acids Res **16:** 10881–10890

DeLille J, Peterson EC, Johnson T, Moore M, Kight A, Henry R (2000) A novel precursor recognition element facilitates posttranslational binding to the signal recognition particle in chloroplasts. Proc Natl Acad Sci USA **97:** 1926–1931

Domon B, Aebersold R (2006) Mass spectrometry and protein analysis. Science **312:** 212–217

Durrett TP, Connolly EL, Rogers EE (2006) Arabidopsis cpFtsY mutants exhibit pleiotropic defects including an inability to increase iron deficiency-inducible root Fe(III) chelate reductase activity. Plant J **47:** 467–479

Eichacker LA, Henry R (2001) Function of a chloroplast SRP in thylakoid protein export. Biochim Biophys Acta **1541:** 120–134

Franklin AE, Hoffman NE (1993) Characterization of a chloroplast homologue of the 54-kDa subunit of the signal recognition particle. J Biol Chem **268:** 22175–22180

Friso G, Giacomelli L, Ytterberg AJ, Peltier JB, Rudella A, Sun Q, Wijk KJ (2004) In-depth analysis of the thylakoid membrane proteome of *Arabidopsis thaliana* chloroplasts: new proteins, new functions, and a plastid proteome database. Plant Cell **16:** 478–499

Froderberg L, Rohl T, van Wijk K, de Gier JL (2001) Complementation of bacterial SecE by a chloroplastic homologue. FEBS Lett **498:** 52–56

Gobom J, Nordhoff E, Mirgorodskaya E, Ekman R, Roepstorff P (1999) Sample purification and preparation technique based on nano-scale reversed-phase columns for the sensitive analysis of complex peptide mixtures by matrix-assisted laser desorption/ionization mass spectrometry. J Mass Spectrom **34:** 105–116

Goshe MB, Smith RD (2003) Stable isotope-coded proteomic mass spectrometry. Curr Opin Biotechnol **14:** 101–109

Hutin C, Havaux M, Carde JP, Kloppstech K, Meiherhoff K, Hoffman N, Nussaume L (2002) Double mutation cpSRP43–/cpSRP54– is necessary to abolish the cpSRP pathway required for thylakoid targeting of the light-harvesting chlorophyll proteins. Plant J **29:** 531–543

Jaru-Ampornpan P, Chandrasekar S, Shan SO (2007) Efficient interaction between two GTPases allows the chloroplast SRP pathway to bypass the requirement for an SRP RNA. Mol Biol Cell **18:** 2636–2645

Jarvis P (2008) Targeting of nucleus-encoded proteins to chloroplasts in plants. New Phytol (in press)

Jarvis P, Robinson C (2004) Mechanisms of protein import and routing in chloroplasts. Curr Biol **14:** R1064–R1077

Jorrin JV, Maldonado AM, Castillejo MA (2007) Plant proteome analysis: a 2006 update. Proteomics **7:** 2947–2962

Kessler F, Schnell DJ (2006) The function and diversity of plastid protein import pathways: a multilane GTPase highway into plastids. Traffic **7:** 248–257

Klimyuk VI, Persello-Cartieaux F, Havaux M, Contard-David P, Schuenemann D, Meiherhoff K, Gouet P, Jones JD, Hoffman NE, Nussaume L (1999) A chromodomain protein encoded by the *Arabidopsis* CAO gene is a plant-specific component of the chloroplast signal recognition particle pathway that is involved in LHCP targeting. Plant Cell **11:** 87–100

Kogata N, Nishio K, Hirohashi T, Kikuchi S, Nakai M (1999) Involvement of a chloroplast homologue of the signal recognition particle receptor protein, FtsY, in protein targeting to thylakoids. FEBS Lett **447:** 329–333

Kovacheva S, Bedard J, Patel R, Dudley P, Twell D, Rios G, Koncz C, Jarvis P (2005) In vivo studies on the roles of Tic110, Tic40 and Hsp93 during chloroplast protein import. Plant J **41:** 412–428

Kovacheva S, Bedard J, Wardle A, Patel R, Jarvis P (2007) Further in vivo studies on the role of the molecular chaperone, Hsp93, in plastid protein import. Plant J **50:** 364–379

Li J, Steen H, Gygi SP (2003) Protein profiling with cleavable isotope-coded affinity tag (cICAT) reagents: the yeast salinity stress response. Mol Cell Proteomics **2:** 1198–1204

Li X, Henry R, Yuan J, Cline K, Hoffman NE (1995) A chloroplast homologue of the signal recognition particle subunit SRP54 is involved in the posttranslational integration of a protein into thylakoid membranes. Proc Natl Acad Sci USA **92:** 3789–3793

Michl D, Robinson C, Shackleton JB, Herrmann RG, Klosgen RB (1994) Targeting of proteins to the thylakoids by bipartite presequences: CFoII is imported by a novel, third pathway. EMBO J **13:** 1310–1317

Mori H, Cline K (2001) Post-translational protein translocation into thylakoids by the Sec and DeltapH-dependent pathways. Biochim Biophys Acta **1541:** 80–90

Nakamura T, Schuster G, Sugiura M, Sugita M (2004) Chloroplast RNA-binding and pentatricopeptide repeat proteins. Biochem Soc Trans **32:** 571–574

Nielsen E, Akita M, Davila-Aponte J, Keegstra K (1997) Stable association of chloroplastic precursors with protein translocation complexes that contain proteins from both envelope membranes and a stromal Hsp 100 molecular chaperone. EMBO J **16:** 935–946

Nilsson R, Brunner J, Hoffman NE, van Wijk KJ (1999) Interactions of ribosome nascent chain complexes of the chloroplast-encoded D1 thylakoid membrane protein with cpSRP54. EMBO J **18:** 733–742

Nilsson R, van Wijk KJ (2002) Transient interaction of cpSRP54 with elongating nascent chains of the chloroplast-encoded D1 protein: 'cpSRP54 caught in the act'. FEBS Lett **524:** 127–133

Niyogi KK, Li XP, Rosenberg V, Jung HS (2005) Is PsbS the site of non-photochemical quenching in photosynthesis? J Exp Bot **56:** 375–382

Peltier JB, Cai Y, Sun Q, Zabrouskov V, Giacomelli L, Rudella A, Ytterberg AJ, Rutschow H, van Wijk KJ (2006) The oligomeric stromal proteome of Arabidopsis thaliana chloroplasts. Mol Cell Proteomics **5:** 114–133

Peltier JB, Emanuelsson O, Kalume DE, Ytterberg J, Friso G, Rudella A, Liberles DA, Soderberg L, Roepstorff P, von Heijne G, et al (2002) Central functions of the lumenal and peripheral thylakoid proteome of *Arabidopsis* determined by experimentation and genome-wide prediction. Plant Cell **14:** 211–236

Pilgrim ML, van Wijk KJ, Parry DH, Sy DA, Hoffman NE (1998) Expression of a dominant negative form of cpSRP54 inhibits chloroplast biogenesis in Arabidopsis. Plant J **13:** 177–186

Pool MR (2005) Signal recognition particles in chloroplasts, bacteria, yeast and mammals. Mol Membr Biol **22:** 3–15

Porra RJ, Thompson WA, Kriedemann PE (1989) Determination of accurate extinction coefficients and simultaneous equations for assaying chlorophylls *a* and *b* extracted with four different solvents: verification of the concentration of chlorophyll standards by atomic absorption spectroscopy. Biochim Biophys Acta **975:** 384–394

Rao D, Momcilovic I, Kobayashi S, Callegari E, Ristic Z (2004) Chaperone activity of recombinant maize chloroplast protein synthesis elongation factor, EF-Tu. Eur J Biochem **271:** 3684–3692

Rohl T, van Wijk KJ (2001) In vitro reconstitution of insertion and processing of cytochrome f in a homologous chloroplast translation system. J Biol Chem **276:** 35465–35472

Sakamoto W (2006) Protein degradation machineries in plastids. Annu Rev Plant Biol **57:** 599–621

Schunemann D (2004) Structure and function of the chloroplast signal recognition particle. Curr Genet **44:** 295–304

Schunemann D (2007) Mechanisms of protein import into thylakoids of chloroplasts. Biol Chem **388:** 907–915

Schuenemann D, Gupta S, Persello-Cartieaux F, Klimyuk VI, Jones JDG, Nussaume L, Hoffman NE (1998) A novel signal recognition particle targets light-harvesting proteins to the thylakoid membranes. Proc Natl Acad Sci USA **95:** 10312–10316

Shevchenko A, Wilm M, Vorm O, Mann M (1996) Mass spectrometric sequencing of proteins silver-stained polyacrylamide gels. Anal Chem **68:** 850–858

Smith PK, Krohn RI, Hermanson GT, Mallia AK, Gartner FH, Provenzano MD, Fujimoto EK, Goeke NM, Olson BJ, Klenk DC (1985) Measurement of protein using bicinchoninic acid. Anal Biochem **150:** 76–85

Soll J, Schleiff E (2004) Protein import into chloroplasts. Nat Rev Mol Cell Biol **5:** 198–208

Sun Q, Emanuelsson O, van Wijk KJ (2004) Analysis of curated and predicted plastid subproteomes of Arabidopsis: subcellular compartmentalization leads to distinctive proteome properties. Plant Physiol **135:** 723–734

Sundberg E, Slagter JG, Fridborg I, Cleary SP, Robinson C, Coupland G (1997) ALBINO3, an *Arabidopsis* nuclear gene essential for chloroplast differentiation, encodes a chloroplast protein that shows homology to proteins present in bacterial membranes and yeast mitochondria. Plant Cell **9:** 717–730

Tao WA, Aebersold R (2003) Advances in quantitative proteomics via stable isotope tagging and mass spectrometry. Curr Opin Biotechnol **14:** 110–118

Thelen JJ, Peck SC (2007) Quantitative proteomics in plants: choices in abundance. Plant Cell **19:** 3339–3346

Thimm O, Blasing O, Gibon Y, Nagel A, Meyer S, Kruger P, Selbig J, Muller LA, Rhee SY, Stitt M (2004) MAPMAN: a user-driven tool to display genomics data sets onto diagrams of metabolic pathways and other biological processes. Plant J **37:** 914–939

Tu CJ, Peterson EC, Henry R, Hoffman NE (2000) The L18 domain of light-harvesting chlorophyll proteins binds to cpSRP43. J Biol Chem **275:** 13187–13190

Tzvetkova-Chevolleau T, Hutin C, Noel LD, Goforth R, Carde JP, Caffarri S, Sinning I, Groves M, Teulon JM, Hoffman NE, et al (2007) Canonical signal recognition particle components can be bypassed for posttranslational protein targeting in chloroplasts. Plant Cell **19:** 1635–1648

van Wijk KJ, Peltier JB, Giacomelli L (2007) Isolation of chloroplast proteins from Arabidopsis thaliana for proteome analysis. Methods Mol Biol **355:** 43–48

Weber AP, Schwacke R, Flugge UI (2005) Solute transporters of the plastid envelope membrane. Annu Rev Plant Biol **56:** 133–164

Ytterberg AJ, Peltier JB, van Wijk KJ (2006) Protein profiling of plastoglobules in chloroplasts and chromoplasts: a surprising site for differential accumulation of metabolic enzymes. Plant Physiol **140:** 984–997

Zhang L, Paakkarinen V, Suorsa M, Aro EM (2001) A SecY homologue is involved in chloroplast-encoded D1 protein biogenesis. J Biol Chem **276:** 37809–37814

Zybailov B, Rutschow H, Friso G, Rudella A, Emanuelsson O, Sun Q, van Wijk KJ (2008) Sorting signals, N-terminal modifications and abundance of the chloroplast proteome. PLoS One **3:** e1994